

Polar Affine Arithmetic: Optimal Affine Approximation and Operation Development for Computation in Polar Form Under Uncertainty

SHOUXIANG WANG and KAI WANG, Tianjin University

LEI WU, Clarkson University

CHENGSHAN WANG, Tianjin University

Uncertainties practically arise from numerous factors, such as ambiguous information, inaccurate model, and environment disturbance. Interval arithmetic has emerged to solve problems with uncertain parameters, especially in the computational process where only the upper and lower bounds of parameters can be ascertained. In rectangular coordinate systems, the basic interval operations and improved interval algorithms have been developed in the numerical analysis. However, in polar coordinate systems, interval arithmetic still suffers from issues of complex computation and overestimation. This article defines a polar affine variable and develops a polar affine arithmetic (PAA) that extends affine arithmetic to the polar coordinate systems, which performs better in many aspects than the corresponding polar interval arithmetic (PIA). Basic arithmetic operations are developed based on the complex affine arithmetic. The Chebyshev approximation theory and the min-range approximation theory are used to identify the best affine approximation. PAA can accurately keep track of the interdependency among multiple variables throughout the calculation procedure, which prominently reduces the solution conservativeness. Numerical examples implemented in MATLAB programs show that, compared with benchmark results from the Monte Carlo method, the proposed PAA ensures completeness of the exact solution and presents a more compact solution region than PIA when dependency exists in the calculation process. Meanwhile, a comparison of affine arithmetic in polar and rectangular coordinates is presented. An application of PAA in circuit analysis is quantitatively presented and potential applications in other research fields involving complex variables in polar form will be gradually developed.

CCS Concepts: • Theory of computation → Numeric approximation algorithms; • Mathematics of computing → Mathematical software performance;

Additional Key Words and Phrases: Affine approximation method, Monte Carlo sample method, operation development, polar affine arithmetic, polar interval arithmetic, uncertainty

ACM Reference format:

Shouxiang Wang, Kai Wang, Lei Wu, and Chengshan Wang. 2019. Polar Affine Arithmetic: Optimal Affine Approximation and Operation Development for Computation in Polar Form Under Uncertainty. *ACM Trans. Math. Softw.* 45, 1, Article 6 (February 2019), 29 pages.

<https://doi.org/10.1145/3274659>

This work was supported in part by the National Natural Science Foundation of China (NSFC 51361135704). This work was also supported in part by the U.S. National Science Foundation grants ECCS-1254310 and PFI: BIC IIP-1534035.

Author's addresses: S. Wang, K. Wang, and C. Wang are with the Key Laboratory of Smart Grid of Ministry of Education, Tianjin University, Tianjin 300072, China; emails: {sxwang, tju337wangkai, cswang}@tju.edu.cn; L. Wu is with the Electrical and Computer Engineering Department, Clarkson University, Potsdam, NY 13699 USA; email: lwu@clarkson.edu.

Permission to make digital or hard copies of all or part of this work for personal or classroom use is granted without fee provided that copies are not made or distributed for profit or commercial advantage and that copies bear this notice and the full citation on the first page. Copyrights for components of this work owned by others than ACM must be honored. Abstracting with credit is permitted. To copy otherwise, or republish, to post on servers or to redistribute to lists, requires prior specific permission and/or a fee. Request permissions from permissions@acm.org.

© 2019 Association for Computing Machinery.

0098-3500/2019/02-ART6 \$15.00

<https://doi.org/10.1145/3274659>

1 INTRODUCTION

In numerical analysis, complex variables can be presented via rectangular, circular, or polar forms. Due to various uncertainties, it may not be practical to obtain exact solutions of variables along the computational process, especially in engineering applications (Wood et al. 1992; Pal and Bezdek 1994). Such uncertainties may arise from various situations such as incompleteness of information (Ferrando 2002), interference in communication (Doerr 2013), inaccuracy of established models (Heupke et al. 2006; Granvilliers and Benhamou 2006), and approximation of algorithms (Piccolo et al. 2013). Alternatively, in many cases, it becomes a necessity to obtain the full range of output variables under uncertainties. Even though certain models and algorithms have been developed in existing studies (Rao et al. 2010; Stol and Figueiredo 1997; Ding et al. 2012; Vaccaro et al. 2010; Wu and Mendel 2002), a common issue is that the calculation procedure is complex and time consuming.

Generally, only the upper and lower bounds of uncertain parameters can be ascertained with the constraints of environment and data source. Under this situation, two commonly used approaches can incorporate such uncertainty information along the calculation procedure. The first approach is the simulation-based algorithm, which approximates ranges of output variables by running model repeatedly with different input values randomly taken from the uncertainty range. Saracco and Pia (2013) study computational issues for quantifying non-statistical uncertainties via numerical Monte Carlo (MC) simulations. The second approach is the interval arithmetic (IA), which has been extended in the complex space. It can evaluate the ranges of output variables efficiently but come with the issue of overestimation. Studies in theory, method, and application of interval analysis are presented in Alefeld and Mayer (2000). Boche (1966) develops complex interval arithmetic and elaborates its potential applications.

Considering uncertainties, a complex interval variable in rectangular form is represented by an axis-aligned rectangle, and the circular form is represented by a disc (Petkovic et al. 1998). Addition and subtraction do not cause difficulties when using complex rectangular or circular interval arithmetic. However, multiplication and division are not exact in these arithmetics (Klatte and Ullrich 1980; Gargantini and Henrici 1971; Farouki and Pottmann 2002). Then, affine arithmetic (AA) is presented in Luiz et al. (1993) as an improved interval method, and its application to computer graphics is introduced. Figueiredo et al. (1997) obtains faster solutions to unconstrained global optimization problems by combining acceleration techniques for interval branch-and-bound methods with AA. Manson (2005) and Wang et al. (2015) extend AA to the complex space and apply it to frequency response as well as uncertainty tracing in power systems. However, the above work only develops AA in rectangular coordinates (RAA). As for operations in RAA, addition and subtraction are relatively easier than multiplication and division. Compared to interval arithmetic in rectangular coordinates, the solution region obtained from RAA is more compact when dependency exists in the calculation process. The use of AA in rectangular coordinates reduces conservativeness due to the ability to keep tracking dependencies. Although AA presents such advantages, the application of AA in polar coordinates has not been developed in existing literature. A traditional method is to convert complex variables in polar form to rectangular form. However, the conversion operation may introduce new approximation errors and increase computational complexity. Thus, it is necessary to extend AA to polar coordinates and develop a complete set of corresponding operations.

Meanwhile, it makes more sense to study magnitudes and angles of complex variables in many situations, such as the steady-state linear circuit analysis. Klatte and Ullrich (1980) studies the sector of circular ring and the inclusion by rectangle and different circles. However, the solution region becomes wider through the inclusion by either rectangle or circle. Flores (1999), Candau

et al. (2006), and Cui and Ngan (2011) define a vector in polar form with interval attributes, which is called a complex fan or a polar complex interval. Polar interval arithmetic (PIA) is developed for providing the smallest complex fan that encloses all possible results, especially in the addition operation. Wang et al. (2006) present an interval power flow analysis method with the complex fan representation for distribution networks. However, although the interval arithmetic in polar form has been developed to certain extent, it still suffers from issues of computational complexity and overestimation. That is, it may cause severe error explosion when the procedure involves a long calculation chain (Moore 1962). PIA is developed based on the assumption that uncertain variables are independent, which may not always hold and in turn could exacerbate the overestimation situation.

This article develops a polar affine arithmetic (PAA) that extends AA to polar coordinate systems. Basic arithmetic operations including addition, subtraction, multiplication, and division are defined, and other operations are developed based on these basic arithmetic operations. The proposed PAA can accurately represent the interdependency among variables and effectively keep track of dependencies along the calculation procedure, which may prominently reduce the solution conservativeness. Furthermore, the computation procedure is more efficient than the PIA and the MC sampling method. The result of the proposed PAA can be directly calculated by affine operations. However, in the addition operation of PIA, certain variables should be first identified for determining the maximum and minimum values of magnitude and angle. Then, extremes of the results can be calculated by the addition operation according to specific variables (Flores 1999; Candau et al. 2006). An MC sampling method is always necessary, which can depict the true solution region through repetitive simulations. Moreover, numerical studies show that the proposed PAA ensures completeness of true solutions and also returns a more compact solution region than PIA when dependency exists in the calculation process. A comparison of affine arithmetic in polar and rectangular coordinates is presented. It is noted that the advantages and disadvantages of using either polar or rectangular form are case specific. Finally, an application in circuit analysis is presented to support directly using PAA in polar coordinate systems.

The rest of the article is organized as follows. The operational rules of PIA are briefly introduced in Section 2. Section 3 provides the definition of a polar affine variable and the conversion between PIA and PAA. Section 4 presents the basic multiplication and division operations, and Section 5 provides the basic addition and subtraction operations in PAA. In both Sections 4 and 5, the results from PAA, PIA, and MC are compared to illustrate the effectiveness and efficiency of the proposed PAA. A comparison of affine arithmetic in polar and rectangular coordinates is provided in Section 6. An application of PAA in circuit analysis is shown in Section 7. Finally, major conclusions are summarized in Section 8.

2 BASIC OPERATIONS FOR POLAR INTERVAL ARITHMETIC

A complex fan variable in interval form is represented as

$$\tilde{x} = [\underline{x}_m, \bar{x}_m] \angle [\underline{x}_\alpha, \bar{x}_\alpha], \quad (1)$$

where $\bar{x}_m/\underline{x}_m$ and $\bar{x}_\alpha/\underline{x}_\alpha$ are the upper/lower bounds of magnitude and angle of \tilde{x} , respectively. Equation (1) describes a semi-circular region spanning over circular segments that is similar to a fan, which is referred to as a complex fan.

Considering two interval variables in polar form $\tilde{x} = [\underline{x}_m, \bar{x}_m] \angle [\underline{x}_\alpha, \bar{x}_\alpha]$ and $\tilde{y} = [\underline{y}_m, \bar{y}_m] \angle [\underline{y}_\alpha, \bar{y}_\alpha]$, the elementary operations are given as follows:

$$\tilde{x} \cdot \tilde{y} = \left([\underline{x}_m, \bar{x}_m] \cdot [\underline{y}_m, \bar{y}_m] \right) \angle \left([\underline{x}_\alpha, \bar{x}_\alpha] + [\underline{y}_\alpha, \bar{y}_\alpha] \right), \quad (2)$$

$$\tilde{x}/\tilde{y} = \left([\underline{x}_m, \bar{x}_m] / [\underline{y}_m, \bar{y}_m] \right) \angle \left([\underline{x}_\alpha, \bar{x}_\alpha] - [\underline{y}_\alpha, \bar{y}_\alpha] \right) \quad (3)$$

$$-\tilde{x} = -[\underline{x}_m, \bar{x}_m] \angle [\underline{x}_\alpha, \bar{x}_\alpha] = [\underline{x}_m, \bar{x}_m] \angle [\underline{x}_\alpha + \pi, \bar{x}_\alpha + \pi]. \quad (4)$$

The basic interval operations used in Equations (2)–(4) are defined as follows:

$$[\underline{x}, \bar{x}] + [\underline{y}, \bar{y}] = [\underline{x} + \underline{y}, \bar{x} + \bar{y}], \quad (5)$$

$$[\underline{x}, \bar{x}] - [\underline{y}, \bar{y}] = [\underline{x} - \bar{y}, \bar{x} - \underline{y}], \quad (6)$$

$$\begin{aligned} [\underline{x}, \bar{x}] \cdot [\underline{y}, \bar{y}] &= [\min(\underline{x} \cdot \underline{y}, \underline{x} \cdot \bar{y}, \bar{x} \cdot \underline{y}, \bar{x} \cdot \bar{y}), \\ &\quad \max(\underline{x} \cdot \underline{y}, \underline{x} \cdot \bar{y}, \bar{x} \cdot \underline{y}, \bar{x} \cdot \bar{y})], \end{aligned} \quad (7)$$

$$[\underline{x}, \bar{x}] / [\underline{y}, \bar{y}] = [\underline{x}, \bar{x}] \cdot [1/\bar{y}, 1/\underline{y}], \quad 0 \notin [\underline{y}, \bar{y}]. \quad (8)$$

One critical difficulty is the complication resided in the addition operation, in terms that no straightforward formula is available to directly perform the calculation. A traditional method is to convert complex variables in polar form to rectangular or circular form, which may derive too conservative results due to the conversion (Klatte and Ullrich 1980). Consequently, PIA is developed as a means for providing the smallest complex fan that encloses all possible results (Flores 1999; Candau et al. 2006).

Interval arithmetic (IA) is a computation model that can manipulate imprecise data and keep track automatically of rounding errors. The interval of each computation result is widened due to the needs for representing its endpoints as floating-point values. The advantage of IA is that the safe direction of rounding can be effectively identified. Indeed, the lower bound is rounded towards $-\infty$ and the upper bound is rounded towards $+\infty$. That is, variables in IA are always rounded in the most conservative direction to guarantee the completeness property of the results.

3 DEFINITION AND CONVERSION OF PAA

3.1 Definition of Polar Affine Arithmetic

A polar affine variable in PAA is defined as

$$\hat{x} = \hat{x}_m \angle \hat{x}_\alpha = \left(x_{m0} + \sum_{i=1}^n x_{mi} \varepsilon_{mi} \right) \angle \left(x_{\alpha 0} + \sum_{i=1}^n x_{\alpha i} \varepsilon_{\alpha i} \right), \quad (9)$$

where represents the magnitude of \hat{x} ; \hat{x}_α represents the angle of \hat{x} ; x_{m0} and $x_{\alpha 0}$ are real numbers representing central values of \hat{x}_m and \hat{x}_α ; $x_{\alpha i}$ and x_{mi} are real coefficients representing the partial deviations; ε_{mi} and $\varepsilon_{\alpha i}$ are noisy symbols lying in the interval $[-1, 1]$.

Considering a complex fan variable in interval form as $\tilde{x} = [1, 5] \angle [\frac{\pi}{9}, \frac{\pi}{3}]$, the interval form is unable to show the dependency between magnitude and angle. Thus, it can be converted into the corresponding affine form as $\hat{x} = (3 + 2\varepsilon_1) \angle (\frac{2}{9}\pi + \frac{\pi}{9}\varepsilon_2)$. Figure 1(a) shows the solution region when there is no dependency between magnitude and angle. The red dot area is the true solution region obtained from the MC sampling method. The complex interval boundary is the same as the complex affine boundary, because no dependency exists in both forms.

When dependency between magnitude and angle exists, it is represented in affine form as $\hat{x} = (3 + \varepsilon_1 - \varepsilon_2) \angle (\frac{2}{9}\pi + \frac{\pi}{9}\varepsilon_2)$. The corresponding complex fan is $\tilde{x} = [1, 5] \angle [\frac{\pi}{9}, \frac{\pi}{3}]$. The solution region is shown in Figure 1(b). The black line is the complex interval boundary and the blue line is the complex affine boundary. The red dot area is the true solution region. The complex affine boundary is closer to the true solution, because it can accurately reflect the correlation information between magnitude and angle. Note that this example considers the dependency between magnitude and angle via a common noisy symbol ε_2 , which is different from the traditional PIA

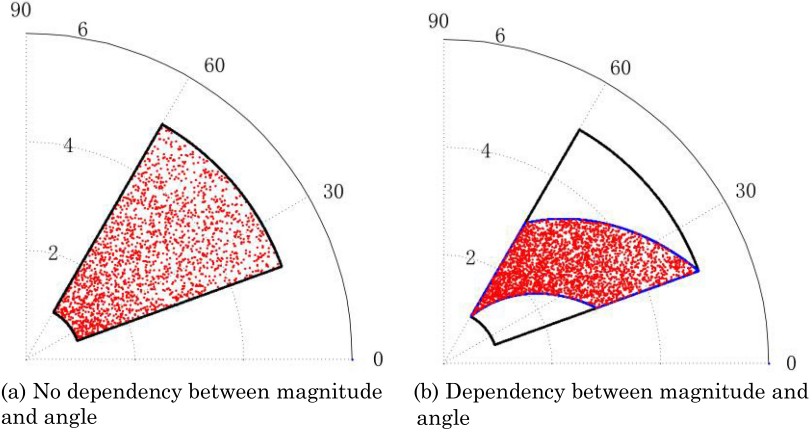


Fig. 1. Comparison of complex affine variable with complex interval variable in polar coordinates.

approach. Points lying on the boundary of the affine region are depicted by varying ε_i over $[-1, 1]$ while fixing the other noisy symbol ε_j as -1 or $+1$.

The main weakness of PIA is the conservativeness, which is mainly caused by the assumption that magnitude and angle of individual variable are independent over the given intervals. That is, the value of angle can vary independently over its entire uncertainty interval with a given value of magnitude. However, the proposed PAA can keep track of dependencies between magnitude and angle of individual variable as well as among multiple variables throughout the calculation procedure. Consequently, the conservativeness is reduced, while all possible solutions are guaranteed to be enclosed in the derived uncertainty interval.

AA presents the same ability as IA to automatically keep track of rounding errors for each computed variable. Given a variable as $\hat{x} = x_0 + x_1\varepsilon_1 + x_2\varepsilon_2 + \dots + x_n\varepsilon_n$, errors derived from the computation function $\hat{z} = f(\hat{x}) = z_0 + z_1\varepsilon_1 + z_2\varepsilon_2 + \dots + z_n\varepsilon_n + z_k\varepsilon_k$ mainly contain the numerical approximation errors and rounding errors, which are combined into a new term $z_k\varepsilon_k$. First, the numerical approximation errors come from the needs to cast the results of non-linear operations as affine forms. Second, the floating-point rounding errors must be considered when computing coefficients of the results.

In IA, endpoints of the results have the safe direction for rounding. However, there is no such a safe direction for rounding the partial deviation z_i in AA. However, the advantage of AA is that the correlation and dependency information can be reflected through common noisy symbols. Thus, different rounding directions of z_i will arouse different correlations among operands. Fortunately, variables in AA present unique advantages for handling rounding errors via the term $z_k\varepsilon_k$. That is, whenever a computed result z_i differs from the true value, the error is handled by adding a distinct term $z_k\varepsilon_k$. Since the new term $z_k\varepsilon_k$ derived from each computation is distinct from existing terms, the coefficient z_k is allowed to round away from zero. Furthermore, all the added terms $z_k\varepsilon_k$ derived from the rounding errors and numerical approximation errors can be combined into a single distinct term, because individual added terms are independent from each other.

3.2 Conversion between PIA and PAA

Let $\tilde{x} = [\underline{x}_m, \bar{x}_m] \angle [\underline{x}_\alpha, \bar{x}_\alpha]$ represent a variable in PIA. It can be converted into an equivalent affine form as $\hat{x} = \hat{x}_m \angle \hat{x}_\alpha$, where

$$\hat{x}_m = \frac{\bar{x}_m + \underline{x}_m}{2} + \frac{\bar{x}_m - \underline{x}_m}{2}\varepsilon_m, \quad (10)$$

$$\hat{x}_\alpha = \frac{\bar{x}_\alpha + \underline{x}_\alpha}{2} + \frac{\bar{x}_\alpha - \underline{x}_\alpha}{2}\varepsilon_\alpha. \quad (11)$$

Given a variable in affine form as in Equation (9), it can be converted into an interval variable as in Equation (1), where

$$\bar{x}_m = x_{m0} + \sum_{i=1}^n |x_{mi}|, \quad (12)$$

$$\underline{x}_m = x_{m0} - \sum_{i=1}^n |x_{mi}|, \quad (13)$$

$$\bar{x}_\alpha = x_{\alpha0} + \sum_{i=1}^n |x_{\alpha i}|, \quad (14)$$

$$\underline{x}_\alpha = x_{\alpha0} - \sum_{i=1}^n |x_{\alpha i}|. \quad (15)$$

Note that the conversion from the affine form to the interval form results in the loss of correlation information among variables.

4 MULTIPLICATION AND DIVISION IN PAA

4.1 Multiplication

Given two polar affine variables \hat{x} and \hat{y} as

$$\hat{x} = \left(x_{m0} + \sum_{i=1}^n x_{mi}\varepsilon_{mi} \right) \angle \left(x_{\alpha0} + \sum_{i=1}^n x_{\alpha i}\varepsilon_{\alpha i} \right) = \hat{x}_m \angle \hat{x}_\alpha, \quad (16)$$

$$\hat{y} = \left(y_{m0} + \sum_{i=1}^n y_{mi}\varepsilon_{mi} \right) \angle \left(y_{\alpha0} + \sum_{i=1}^n y_{\alpha i}\varepsilon_{\alpha i} \right) = \hat{y}_m \angle \hat{y}_\alpha, \quad (17)$$

the multiplication operation in PAA is defined as

$$\hat{z} = \hat{x} \times \hat{y} = (\hat{x}_m \times \hat{y}_m) \angle (\hat{x}_\alpha + \hat{y}_\alpha) = \hat{z}_m \angle \hat{z}_\alpha, \quad (18)$$

where $\hat{z}_\alpha = \hat{x}_\alpha + \hat{y}_\alpha = x_{\alpha0} + y_{\alpha0} + \sum_{i=1}^n (x_{\alpha i} + y_{\alpha i})\varepsilon_{\alpha i}$, and $\hat{z}_m = \hat{x}_m \times \hat{y}_m$.

\hat{z}_m is the affine expression of the product of \hat{x}_m and \hat{y}_m . The exact expression z_m is calculated as in Equation (19):

$$\begin{aligned} z_m &= \hat{x}_m \times \hat{y}_m \\ &= x_{m0}y_{m0} + \sum_{i=1}^n (x_{m0}y_{mi} + y_{m0}x_{mi})\varepsilon_{mi} + \left(\sum_{i=1}^n x_{mi}\varepsilon_{mi} \right) \cdot \left(\sum_{i=1}^n y_{mi}\varepsilon_{mi} \right). \end{aligned} \quad (19)$$

Since the first two terms in Equation (19) are already in affine form, the main purpose is to find the affine approximation for the last term. Equation (20) is a simple affine approximation presented by Comba and Stolfi, which may derive conservative results:

$$\begin{aligned} \hat{z}_m &= \hat{x}_m \times \hat{y}_m \\ &= x_{m0}y_{m0} + \sum_{i=1}^n (x_{m0}y_{mi} + y_{m0}x_{mi})\varepsilon_{mi} + \left(\sum_{i=1}^n |x_{mi}| \right) \cdot \left(\sum_{i=1}^n |y_{mi}| \right) \varepsilon_k, \end{aligned} \quad (20)$$

where ε_k is a completely independent noisy symbol lying in $[-1, 1]$.

This article adopts a better affine approximation method for multiplication as shown in Equation (21). The new approximation method aims to reduce the overestimation while guaranteeing

the completeness of true solutions. First, the first two terms of the exact expression as in Equation (19) are retained in both Equations (20) and (21). Second, as for components $x_{mi}y_{mi}\varepsilon_{mi}^2$ contained in the third term of Equation (19), true solutions lie in the interval $[0, x_{mi}y_{mi}]$ due to the square operation (ε_{mi}^2). The approximation in Equation (21) returns the results varying between 0 and $x_{mi}y_{mi}$ as compared to $-x_{mi}y_{mi}$ and $x_{mi}y_{mi}$ obtained from Equation (20). Third, as for components $x_{mi}y_{mj}\varepsilon_{mi}\varepsilon_{mj}$ ($i \neq j$) in the third term of Equation (19), the previous method directly approximates it by summing absolute values of individual terms ($|x_{mi}y_{mj}|$) as shown in Equation (20). In comparison, the new method primarily merges the terms with the same noisy symbol ($\varepsilon_{mi}\varepsilon_{mj}$) and consequently the approximation is carried out by summing absolute values of individual terms ($|x_{mi}y_{mj} + x_{mj}y_{mi}|$) as shown in Equation (21). Such a grouping reduces conservativeness of the results, while the summation of absolute values also ensures the completeness of true solutions. Overall, the new approximation method reduces the overestimation while also avoiding underestimating the error:

$$\begin{aligned}\hat{z}_m = \hat{x}_m \times \hat{y}_m &= x_{m0}y_{m0} + \frac{1}{2} \sum_{i=1}^n x_{mi}y_{mi} + \sum_{i=1}^n (x_{m0}y_{mi} + y_{m0}x_{mi})\varepsilon_{mi} \\ &+ \left(\frac{1}{2} \sum_{i=1}^n |x_{mi}y_{mi}| + \sum_{i=1}^n \sum_{j=i+1}^n |(x_{mi}y_{mj} + x_{mj}y_{mi})| \right) \varepsilon_k.\end{aligned}\quad (21)$$

MATLAB Code for Multiplication in PAA

```
function [multimag,multiang]=multiplication(xmag,xang,ymag,yang)
%calculate the number of noisy symbols
xmnum=length(xmag);xanum=length(xang);
ymnum=length(ymag);yanum=length(yang);
for i=1:min(xanum,yanum) %calculate angle of the result
    multiang(i)=xang(i)+yang(i);
end
if xanum>yanum
    for i=min(xanum,yanum)+1:1:xanum
        multiang(i)=xang(i);
    end
else if xanum<yanum
    for i=min(xanum,yanum)+1:1:yanum
        multiang(i)=yang(i);
    end
end
if xmnum>ymnum %calculate magnitude of the result
    for i=ymnum+1:1:xmnum
        ymag(i)=0;
    end
else if xmnum<ymnum
    for i=xmnum+1:1:ymnum
        xmag(i)=0;
    end
end
end
sum=0;sum1=0;sum2=0;
% calculate central value of the magnitude
for i=2:1:max(xmnum,ymnum)
    sum=sum+xmag(i)*ymag(i);
end
multimag(1)=xmag(1)*ymag(1)+0.5*sum;
%calculate coefficients of the magnitude
for i=2:1:max(xmnum,ymnum)
    multimag(i)=xmag(1)*ymag(i)+xmag(i)*ymag(1);
end
%calculate the error term
for i=2:1:max(xmnum,ymnum)
    sum1=sum1+0.5*abs(xmag(i)*ymag(i));
end
for i=2:1:max(xmnum,ymnum)
    for j=i+1:1:max(xmnum,ymnum)
        sum2=sum2+abs(xmag(i)*ymag(j)+xmag(j)*ymag(i));
    end
end
multimag(max(xmnum,ymnum)+1)=sum1+sum2;
```

Example 4.1. To compare the results of multiplication in PAA and PIA, four cases are implemented to show how the method performs when there is (i) no dependency, (ii) no dependency between the operands but dependency between magnitude and angle, (iii) dependency between the operands but no dependency between magnitude and angle, and (iv) dependencies everywhere.

In case 1, two complex fan variables are given as $\tilde{x} = [2, 6] \angle [\frac{\pi}{36}, \frac{5\pi}{36}]$ and $\tilde{y} = [6, 10] \angle [\frac{\pi}{6}, \frac{5\pi}{18}]$, since there is no dependency. Thus, the corresponding complex affine variables are given as $\hat{x} = (4 + 2\varepsilon_1) \angle (\frac{\pi}{12} + \frac{\pi}{18}\varepsilon_2)$ and $\hat{y} = (8 + 2\varepsilon_3) \angle (\frac{2\pi}{9} + \frac{\pi}{18}\varepsilon_4)$.

Using PIA, the results of multiplication can be calculated as in Equation (22):

$$\tilde{z} = [12, 60] \angle \left[\frac{7\pi}{36}, \frac{5\pi}{12} \right]. \quad (22)$$

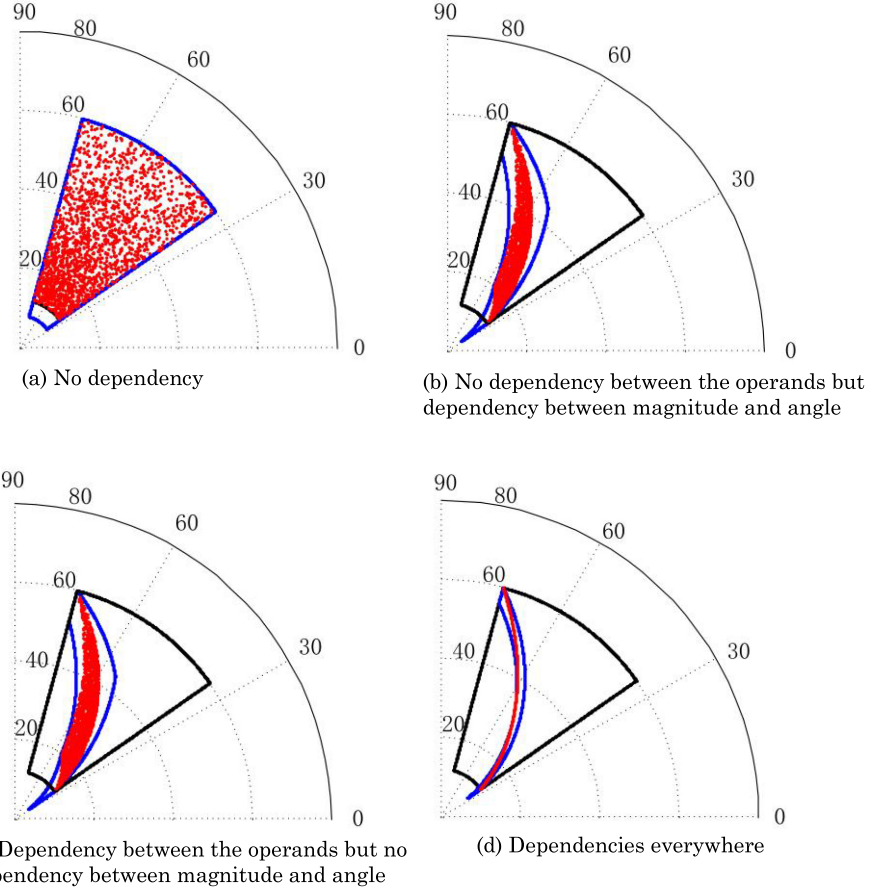


Fig. 2. Results of multiplication in PAA (blue line), PIA (black line), and actual solution (red dot).

Using PAA, the affine approximation for the multiplication of \hat{x} and \hat{y} is given as in Equation (23):

$$\hat{z} = (32 + 16\epsilon_1 + 8\epsilon_3 + 4\epsilon_5) \angle \left(\frac{11\pi}{36} + \frac{\pi}{18}\epsilon_2 + \frac{\pi}{18}\epsilon_4 \right). \quad (23)$$

The results of multiplication in PAA, PIA, and MC simulation are shown in Figure 2(a).

In case 2, there is no dependency between the operands, but dependency between magnitude and angle in each operand exists. The two complex affine variables are given as $\hat{x} = (4 + 2\epsilon_1) \angle (\frac{\pi}{12} + \frac{\pi}{18}\epsilon_1)$ and $\hat{y} = (8 + 2\epsilon_2) \angle (\frac{2\pi}{9} + \frac{\pi}{18}\epsilon_2)$. Since PIA is unable to reflect correlation information, the corresponding complex fan variables are the same as those in case 1.

The affine approximation for the multiplication of \hat{x} and \hat{y} is given as in Equation (24). The results of multiplication in PAA, PIA, and MC simulation are shown in Figure 2(b):

$$\hat{z} = (32 + 16\epsilon_1 + 8\epsilon_2 + 4\epsilon_3) \angle \left(\frac{11\pi}{36} + \frac{\pi}{18}\epsilon_1 + \frac{\pi}{18}\epsilon_2 \right). \quad (24)$$

In case 3, there is dependency between the operands, but no dependency between magnitude and angle in each operand exists. The two complex affine variables are given as $\hat{x} = (4 + 2\epsilon_1) \angle (\frac{\pi}{12} + \frac{\pi}{18}\epsilon_2)$ and $\hat{y} = (8 + 2\epsilon_2) \angle (\frac{2\pi}{9} + \frac{\pi}{18}\epsilon_1)$. The affine approximation for the multiplication of \hat{x} and \hat{y} is

given as in Equation (25). The results of multiplication in PAA, PIA, and MC simulation are shown in Figure 2(c):

$$\hat{z} = (32 + 16\epsilon_1 + 8\epsilon_2 + 4\epsilon_3) \angle \left(\frac{11\pi}{36} + \frac{\pi}{18}\epsilon_1 + \frac{\pi}{18}\epsilon_2 \right). \quad (25)$$

In case 4, dependencies exist in both magnitude and angle. The two complex affine variables are given as $\hat{x} = (4 + 2\epsilon_1) \angle (\frac{\pi}{12} + \frac{\pi}{18}\epsilon_1)$ and $\hat{y} = (8 + 2\epsilon_1) \angle (\frac{2\pi}{9} + \frac{\pi}{18}\epsilon_1)$. The affine approximation for the multiplication of \hat{x} and \hat{y} is given as in Equation (26). The results of multiplication in PAA, PIA, and MC simulation are shown in Figure 2(d):

$$\hat{z} = (34 + 24\epsilon_1 + 2\epsilon_2) \angle \left(\frac{11\pi}{36} + \frac{\pi}{9}\epsilon_1 \right). \quad (26)$$

As shown in Figure 2, the boundaries of solution regions of PAA and PIA are represented in blue line and black line, respectively. The true solution region is obtained from MC simulation as shown in red dot areas. Errors are inevitable in the calculation process due to affine approximations for non-affine operations, including $\epsilon_i\epsilon_j$, ϵ_i^2 , reciprocal, square, square root, as well as trigonometric and anti-trigonometric operations, and so on. Variables in PAA are represented in Equation (9), which is a linear expression in affine form. The linear expression contributes to the unified calculation and low complexity of PAA. Especially when dependency exists in the calculation process, PAA performs better than PIA as shown in Figures 2(b)–2(d). Meanwhile, Figure 2(a) shows that PIA performs better when the two operands are fully independent in a single multiplication, which can also be found in Equations (22) and (23). It is mainly due to affine approximations for the third term ($\epsilon_i\epsilon_j$, ϵ_i^2) in Equation (19). However, cases with fully independent variables and calculations are very rare in practice. Indeed, dependencies in calculations among multiple variables widely exist (e.g., $x-x$, x/x , $x(x+y)$). Especially in long calculation chains, dependency is widespread. In addition, the solution region of PIA is a complex fan with four fixed endpoints, while the solution region of PAA presents the similar shape of the corresponding true solution region. Compared to PIA, the superiority becomes more obvious especially when dependencies in the calculation process become stronger.

It is noted that the solution region can indeed become better with the intersection of PIA and PAA. However, this article aims at extending AA to polar coordinates and developing a complete set of operations in PAA. The complexity and precision of PAA have been clarified by comprehensive comparisons. The intersection of PIA and PAA will require two sets of algorithms in the calculation process, which largely increases the complexity. Moreover, compared with PIA, PAA performs better most of the time especially when dependency exists. In long calculation chains described above, directly using PAA performs well with satisfactory precision and appropriate complexity.

4.2 Division

Given two polar affine variables \hat{x} and \hat{y} as in Equation (9), we develop the division operation as

$$\hat{z} = \hat{x}/\hat{y} = (\hat{x}_m/\hat{y}_m) \angle (\hat{x}_\alpha - \hat{y}_\alpha) = \hat{z}_m \angle \hat{z}_\alpha, \quad (27)$$

where

$$\hat{z}_\alpha = \hat{x}_\alpha - \hat{y}_\alpha = x_{\alpha 0} - y_{\alpha 0} + \sum_{i=1}^n (x_{\alpha i} - y_{\alpha i})\epsilon_{\alpha i}, \quad (28)$$

$$\hat{z}_m = \hat{x}_m/\hat{y}_m = \hat{x}_m \times \frac{1}{\hat{y}_m}. \quad (29)$$

As the multiplication operation has already been defined, we only need to develop the reciprocal operation to perform the above calculation.

Since affine approximations for non-affine operations in the calculation process are inevitable, this article makes efforts to find optimal affine approximations based on the Chebyshev approximation theory and the min-range approximation theory. The solution regions of these approximations require compact boundaries while guaranteeing completeness of the true solutions. Given a polar affine variable \hat{x} as in Equation (9), it can be converted to the corresponding polar interval form as $\tilde{x} = [a, b](0 \notin \tilde{x})$. The Chebyshev approximation method is adopted for calculating $\hat{z} = 1/\hat{x}$ over the above interval range.

The Chebyshev approximation theory is an approximation method to minimize the maximum absolute error (Stol and Figueiredo 1997). As for function $z = f(x, y)$, the affine approximation to f is of the form $\hat{z} = \alpha\hat{x} + \beta\hat{y} + \xi + z_k\varepsilon_k$, which is the affine combination of \hat{x} and \hat{y} . As for a univariate function $z = f(x)$, the best affine approximation to f is indeed of the form $\hat{z} = \alpha\hat{x} + \xi + z_k\varepsilon_k$. Two error measures are used to verify the accuracy. (1) We can measure the error by the magnitude of coefficient z_k . This value measures the uncertainty in the true value of z that the affine form \hat{z} allows but fails to catch considering uncertainties. (2) We can use the volume of the polytope P_{xyz} jointly determined by the affine forms of \hat{x} , \hat{y} , and $\hat{z} = f(\hat{x}, \hat{y})$. This value measures the uncertainty in the location of point (x, y, z) . Fortunately, it turns out that the two error measures are equivalent and minimizing the volume of P_{xyz} is equivalent to minimizing $|z_k|$. Thus, the Chebyshev approximation, which minimizes the maximum absolute error $|z_k|$, complies with this situation and can be adopted to identify the optimum affine approximations for non-affine functions $z = f(x)$ ($1/x$, $\sin x$, $\cos x$, etc.). Specifically, for univariate functions, the Chebyshev approximation theory presents important properties as follows.

THEOREM 1. *Function f is a bounded and continuous function from a closed and bounded interval $I = [a, b]$ to R . Function g is the affine function that best approximates f in I while satisfying the minimax error criterion. There exists three distinct points u , v , and w in I , where the error $f(x) - g(x)$ has the maximum magnitude; and the sign of error alternates when these three points are in an ascending order.*

THEOREM 2. *Function f is a bounded and twice differentiable function defined on the interval $I = [a, b]$, whose sign of the second derivative f'' does not change in I . Let $f^a = \alpha x + \xi$ be the minimax affine approximation in I . Then*

- (1) *The coefficient α is $(f(b) - f(a))/(b - a)$, which is the slope of line $r(x)$ that interpolates points $(a, f(a))$ and $(b, f(b))$.*
- (2) *The maximum absolute error will appear twice (with the same sign) at the endpoints a and b , and once (with the opposite sign) at every interior point u of I where $f'(u) = \alpha$.*
- (3) *The independent term ξ is $\alpha u + \xi = (f(u) + r(u))/2$, and the maximum absolute error δ is $|f(u) - r(u)|/2$.*

The affine form of the reciprocal obtained from the Chebyshev approximation method is shown as

$$\hat{z} = \frac{1}{\hat{x}} = \alpha\hat{x} + \beta + \delta\varepsilon_k, \quad (30)$$

where

$$\alpha = -\frac{1}{ab}, \quad (31)$$

$$\beta = \frac{1}{2a} + \frac{1}{2b} + \frac{1}{\sqrt{ab}}, \quad (32)$$

$$\delta = \left| \frac{1}{2a} + \frac{1}{2b} - \frac{1}{\sqrt{ab}} \right|. \quad (33)$$

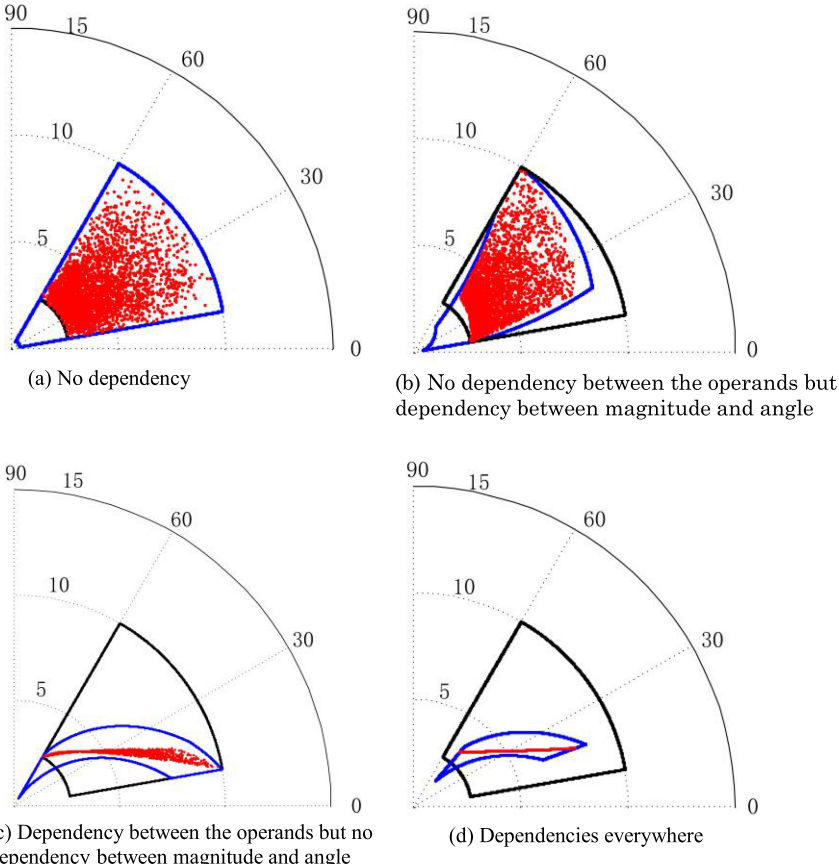


Fig. 3. Results of division in PAA (blue line), PIA (black line), and actual solution (red dot).

MATLAB Code for Division in PAA

```
function [divmag,divang]=division(xmag,xang,ymag,yang)
recm=reciprocal(ymag); %calculate magnitude of the reciprocal of y
reca=-yang; %calculate angle of the reciprocal of y
[divmag,divang]=multiplication(xmag,xang,recm,reca); %calculate the multiplication of x and the reciprocal of y
```

Example 4.2. To compare the results of division in PAA and PIA, four cases are implemented to show how the methods perform in the same way as example 4.1.

In case 1, two complex fan variables are given as $\tilde{x} = [8, 10] \angle [\frac{\pi}{6}, \frac{7\pi}{18}]$ and $\tilde{y} = [1, 3] \angle [\frac{\pi}{18}, \frac{\pi}{9}]$, since there is no dependency. Thus, the corresponding complex affine variables are given as $\hat{x} = (9 + \varepsilon_1) \angle (\frac{5\pi}{18} + \frac{\pi}{9}\varepsilon_2)$ and $\hat{y} = (2 + \varepsilon_3) \angle (\frac{\pi}{12} + \frac{\pi}{36}\varepsilon_4)$.

Using PIA, the results of division can be calculated as in Equation (34):

$$\tilde{z} = \left[\frac{8}{3}, 10 \right] \angle \left[\frac{\pi}{18}, \frac{\pi}{3} \right]. \quad (34)$$

Using PAA, the polar affine approximation for the division of \hat{x} and \hat{y} is calculated as

$$\hat{z} = (5.1966 + 0.5774\varepsilon_1 - 2.9997\varepsilon_3 + 1.2263\varepsilon_5) \angle \left(\frac{7\pi}{36} + \frac{\pi}{9}\varepsilon_2 - \frac{\pi}{36}\varepsilon_4 \right). \quad (35)$$

The results of division in PAA, PIA, and MC simulation are shown in Figure 3(a).

In case 2, there is no dependency between the operands, but dependency between magnitude and angle in each operand exists. Two complex affine variables are given as $\hat{x} = (9 + \varepsilon_1) \angle (\frac{5\pi}{18} + \frac{\pi}{9}\varepsilon_1)$ and $\hat{y} = (2 + \varepsilon_2) \angle (\frac{\pi}{12} + \frac{\pi}{36}\varepsilon_2)$. The corresponding complex fan variables are the same as case 1.

The affine approximation for the division of \hat{x} and \hat{y} is given as in Equation (36). The results of division in PAA, PIA, and MC simulation are shown in Figure 3(b):

$$\hat{z} = (5.1966 + 0.5774\varepsilon_1 - 2.9997\varepsilon_2 + 1.2263\varepsilon_3) \angle \left(\frac{7\pi}{36} + \frac{\pi}{9}\varepsilon_1 - \frac{\pi}{36}\varepsilon_2 \right). \quad (36)$$

In case 3, there is dependency between the operands, but no dependency between magnitude and angle in each operand exists. Two complex affine variables are given as $\hat{x} = (9 + \varepsilon_1) \angle (\frac{5\pi}{18} + \frac{\pi}{9}\varepsilon_1)$ and $\hat{y} = (2 + \varepsilon_2) \angle (\frac{\pi}{12} + \frac{\pi}{36}\varepsilon_1)$. The affine approximation for the division of \hat{x} and \hat{y} is given as in Equation (37). The results of division in PAA, PIA, and MC simulation are shown in Figure 3(c):

$$\hat{z} = (5.1966 + 0.5774\varepsilon_1 - 2.9997\varepsilon_2 + 1.2263\varepsilon_3) \angle \left(\frac{7\pi}{36} - \frac{\pi}{36}\varepsilon_1 + \frac{\pi}{9}\varepsilon_2 \right). \quad (37)$$

In case 4, dependencies exist in both magnitude and angle. Two complex affine variables are given as $\hat{x} = (9 + \varepsilon_1) \angle (\frac{5\pi}{18} + \frac{\pi}{9}\varepsilon_1)$ and $\hat{y} = (2 + \varepsilon_1) \angle (\frac{\pi}{12} + \frac{\pi}{36}\varepsilon_1)$. The affine approximation for the division of \hat{x} and \hat{y} is given as in Equation (38). The results of division in PAA, PIA, and MC simulation are shown in Figure 3(d):

$$\hat{z} = (5.0300 - 2.4223\varepsilon_1 + 1.0597\varepsilon_2) \angle \left(\frac{7\pi}{36} + \frac{\pi}{12}\varepsilon_1 \right). \quad (38)$$

In Figure 3, the boundaries of solution regions of PAA and PIA are represented in blue line and black line, respectively. The true solution region obtained from MC simulation is also shown in red dot areas. In Figure 3(a), to obtain the linear approximation for division in affine form with no dependency, the range of magnitude becomes wider. When dependency exists in cases 2–4, it demonstrates that the solution region of PAA is much closer to the true solution region than that of PIA because of its capability of keeping track of dependency in calculation process. Thus, PAA reduces the conservativeness incurred by PIA when dependency exists. Compared to PIA, the superiority of division in PAA becomes more significant as the degree of dependency becomes larger. The solution region of PAA also presents a similar shape as that of the true solution region.

5 ADDITION AND SUBTRACTION IN PAA

5.1 Negation

Given a polar affine variable as in Equation (9), we define the negation operation as

$$\begin{aligned} \hat{z} &= -\hat{x} = \left(x_{m0} + \sum_{i=1}^n x_{mi}\varepsilon_{mi} \right) \angle \left(x_{\alpha 0} + \pi + \sum_{i=1}^n x_{\alpha i}\varepsilon_{\alpha i} \right) \\ &= \hat{x}_m \angle (\hat{x}_\alpha + \pi). \end{aligned} \quad (39)$$

That is, the negative value of a polar affine variable has the same magnitude and complementary angle to the original one.

5.2 Subtraction

The subtraction operation can be defined in terms of addition and negation as

$$\hat{z} = \hat{x} - \hat{y} = \hat{x} + (-\hat{y}). \quad (40)$$

Since the negation operation has already been discussed in Equation (39), we define the addition operation as follows.

5.3 Addition

In complex plane, the addition operation in PAA is a complicated issue and still lacks an explicit and efficient formula in polar form. Indeed, numerous trigonometry operations increase the complication to a large extent. This article proposes an algorithm based on the Chebyshev approximation theory and the min-range approximation theory to explore the addition operation in PAA.

5.3.1 Decomposition. It is important to maintain the concavity and convexity of functions along the calculation procedure. Thus, we first decompose the solution region of each polar affine variable into four quadrants. For instance, the polar affine variable can be represented as

$$\hat{x} = \bigcup_{i=1,2,3,4} \hat{x}_i, \quad (41)$$

where

$$\hat{x}_i = (0, +\infty) \angle [90(i-1), 90i] \cap \hat{x}. \quad (42)$$

The addition operation of two polar affine variables can be expressed as

$$\begin{aligned} \hat{z} &= \hat{x} + \hat{y} \\ &= (\hat{x}_1 \cup \hat{x}_2 \cup \hat{x}_3 \cup \hat{x}_4) + (\hat{y}_1 \cup \hat{y}_2 \cup \hat{y}_3 \cup \hat{y}_4) \\ &= \{v + w \mid (v, w) \in (\hat{x}_1 \cup \hat{x}_2 \cup \hat{x}_3 \cup \hat{x}_4) \times (\hat{y}_1 \cup \hat{y}_2 \cup \hat{y}_3 \cup \hat{y}_4)\}. \end{aligned} \quad (43)$$

Using the distributive law of Cartesian product, Equation (43) can be represented as

$$\begin{aligned} \hat{z} &= \{v + w \mid (v, w) \in \hat{x}_1 \times \hat{y}_1 \cup \hat{x}_1 \times \hat{y}_2 \cup \dots\} \\ &= \bigcup_{i,j=1,2,3,4} \hat{x}_i + \hat{y}_j. \end{aligned} \quad (44)$$

A major advantage of PAA is that we only need to explore the addition operation in the first quadrant, as the additional operation in the other three quadrants can be equivalently transformed into the first quadrant via the trigonometric function transformations. The final result is the union of all partial results.

5.3.2 Selecting the best Affine Approximation. Considering the addition of the two polar affine variables ($z = \hat{x} + \hat{y}$), the magnitude and angle of z can be obtained by algebraic operation as

$$z_m = \sqrt{\hat{x}_m^2 + \hat{y}_m^2 + 2\hat{x}_m\hat{y}_m \cos \hat{\theta}}, \quad (45)$$

$$z_\alpha = \tan^{-1} \left(\frac{\hat{x}_m \sin \hat{x}_\alpha + \hat{y}_m \sin \hat{y}_\alpha}{\hat{x}_m \cos \hat{x}_\alpha + \hat{y}_m \cos \hat{y}_\alpha} \right), \quad (46)$$

$$\hat{\theta} = \hat{x}_\alpha - \hat{y}_\alpha. \quad (47)$$

To get the affine variable \hat{z} in polar form, the key point is to develop the appropriate polar affine forms \hat{z}_m and \hat{z}_α of z_m and z_α .

(1) Affine approximation for square function

Given an affine variable \hat{x} in polar form, it can be converted to the corresponding interval form as $\tilde{x} = [a, b]$. The Chebyshev approximation for the square operation $z = x^2$ is given by

$$\hat{z} = \alpha \hat{x} + \beta + \delta \varepsilon_k, \quad (48)$$

where

$$\alpha = a + b, \quad (49)$$

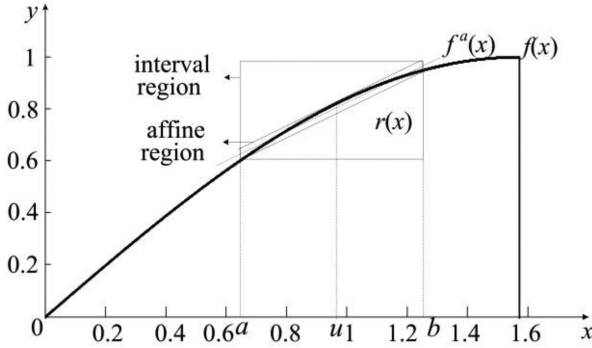


Fig. 4. Affine approximation for $y = \sin x$.

$$\beta = -\frac{ab}{2} - \frac{(a+b)^2}{8}, \quad (50)$$

$$\delta = \left| \frac{ab}{2} - \frac{(a+b)^2}{8} \right|. \quad (51)$$

(2) Affine approximation for square-root function

The Chebyshev approximation for the squared root operation $z = \sqrt{x}$ has the same form as Equation (48) with parameters α , β , and δ calculated as

$$\alpha = \frac{1}{\sqrt{a} + \sqrt{b}}, \quad (52)$$

$$\beta = \frac{\sqrt{a} + \sqrt{b}}{8} + \frac{1}{2} \frac{\sqrt{a}\sqrt{b}}{\sqrt{a} + \sqrt{b}}, \quad (53)$$

$$\delta = \left| \frac{1}{8} \frac{(\sqrt{b} - \sqrt{a})^2}{\sqrt{a} + \sqrt{b}} \right|. \quad (54)$$

(3) Affine approximation for trigonometric and anti-trigonometric functions

No previous work provides specific formula of the affine approximation for trigonometric and anti-trigonometric functions, which present distinct properties of periodicity, concavity, and convexity. As shown in Equations (45)–(47), the operations contain many non-affine functions such as trigonometric, anti-trigonometric, square, and square root, which can bring significant challenges to the calculation procedure.

(1) Affine approximation for Sinusoidal function

Figure 4 shows function $f(x) = \sin(x)$ over the range of $x = [0, \pi/2]$. The challenge is to explore the optimal affine approximation for the non-affine function

$$\begin{aligned} f(\hat{x}) &= \sin(\hat{x}) \\ &= \sin(x_0 + x_1 \varepsilon_1 + x_2 \varepsilon_2 + \dots + x_n \varepsilon_n). \end{aligned} \quad (55)$$

The best affine approximation $f^a(x)$ is developed based on the Chebyshev approximation theory, which is to minimize the maximum absolute error. Since this univariate function is monotonous and concave over the range $[0, \pi/2]$, the best affine approximation has the form of

$$\alpha\hat{x} + \beta = \alpha(x_0 + x_1\varepsilon_1 + \dots + x_n\varepsilon_n) + \beta. \quad (56)$$

According to Theorem 2, α is the slope of line $r(x)$ that goes through points $(a, \sin a)$ and $(b, \sin b)$, which can be calculated as

$$\alpha = \frac{\sin b - \sin a}{b - a}. \quad (57)$$

Thus, line $r(x)$ can be expressed as

$$r(x) = \alpha x + \sin a - \alpha a. \quad (58)$$

The point u at which the slope of the curve is equal to α is calculated as

$$u = \arccos \frac{\sin b - \sin a}{b - a} = \arccos \alpha. \quad (59)$$

Then, the independent term β is calculated as

$$\beta = \frac{f(u) + r(u)}{2} - \alpha u = \frac{1}{2}(\sin u + \sin a - \alpha a - \alpha u). \quad (60)$$

The maximum absolute error δ is calculated as

$$\delta = \frac{|f(u) - r(u)|}{2} = \frac{1}{2}(\sin u - \sin a + \alpha a - \alpha u). \quad (61)$$

Finally, the final affine approximation for function $z = \sin x$ is calculated as

$$\hat{z} = z_0 + z_1\varepsilon_1 + \dots + z_n\varepsilon_n + z_k\varepsilon_k, \quad (62)$$

where

$$z_0 = \alpha x_0 + \beta, \quad (63)$$

$$z_i = \alpha x_i \quad (i = 1, 2, \dots, n), \quad (64)$$

$$z_k = \delta. \quad (65)$$

As shown in Figure 4, the solution region given by the affine arithmetic is much closer to the actual curve than that obtained by the interval arithmetic. Moreover, the affine arithmetic represents the optimal linear approximation for the non-affine function $y = \sin x$ over the interval range $[0, \pi/2]$, which accurately reflects the dependency between input and output variables.

(2) Affine approximation for cosine function

For a univariate function $f(x) = \cos(x)$ over the interval range $x = [0, \pi/2]$, the corresponding interval form of affine variable $\hat{x} = x_0 + \sum_{i=1}^n x_i\varepsilon_i$ is $\tilde{x} = [a, b]$. Using the similar approach applied for function $f(x) = \sin(x)$, the final affine expression has the same form as Equation (62) with parameters given by

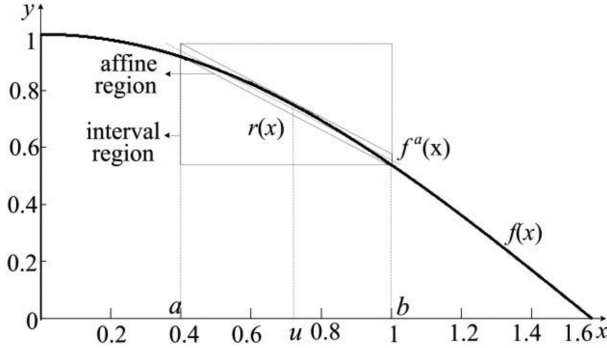
$$z_0 = \alpha x_0 + \beta, \quad (66)$$

$$\alpha = \frac{\cos b - \cos a}{b - a}, \quad (67)$$

$$\beta = (\cos u + \cos a - \alpha a - \alpha u)/2, \quad (68)$$

$$z_i = \alpha x_i \quad (i = 1, 2, \dots, n), \quad (69)$$

$$u = \arcsin(-\alpha), \quad (70)$$

Fig. 5. Affine approximation for $y = \cos x$.

$$z_k = \delta, \quad (71)$$

$$\delta = (\cos u - \cos a + \alpha a - \alpha u)/2. \quad (72)$$

Figure 5 shows similar advantages of the affine arithmetic as observed in Figure 4, which can approximate the actual curve more accurately than the interval arithmetic and also effectively reflect the dependency between input and output variables.

(3) Affine approximation for arctan function

This section discusses, for a certain variable in affine form \hat{x} and the corresponding interval form $\tilde{x} = [a, b]$, how to obtain the affine form as in Equation (62) for the arctan function. The arctan function in PAA is the last but critical step to obtain the angle of the final result for the addition operation. For a polar affine variable \hat{x} ($0 \in \hat{x}$), the Chebyshev approximation theory is no longer applicable, because the concavity and convexity property will change over the range of \hat{x} . Thus, the following two cases are discussed to explore the best affine approximation for the arctan function, by combining the Chebyshev approximation theory with the min-range approximation theory.

Case 1: $0 \notin [a, b]$. This case represents the situation that the entire interval is either in the first or the third quadrant. That is, the concavity and convexity property of the function does not change, and in turn the Chebyshev approximation theory still works. The results have the same form as Equation (62) with parameters calculated via Equations (73)–(76).

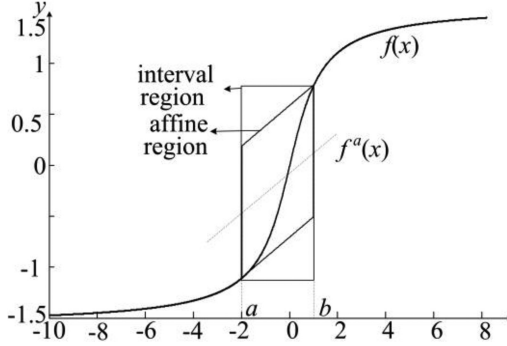
$$\alpha = \frac{\arctan b - \arctan a}{b - a}, \quad (73)$$

$$u = \begin{cases} \sqrt{1/\alpha - 1} & (b > a > 0) \\ -\sqrt{1/\alpha - 1} & (0 > b > a) \end{cases}, \quad (74)$$

$$\beta = (\arctan u + \arctan a - \alpha u - \alpha a)/2, \quad (75)$$

$$\delta = \begin{cases} (\arctan u - \arctan a - \alpha u + \alpha a)/2 & (b > a > 0) \\ (\arctan a - \arctan u + \alpha u - \alpha a)/2 & (0 > b > a) \end{cases}. \quad (76)$$

Case 2: $0 \in [a, b]$. In this case, the curve goes through the point $(0, 0)$, which in turn changes the concavity and convexity property. Thus, the Chebyshev approximation theory cannot be applied in this case. The min-range approximation theory is adopted to explore the affine form of arctan function instead.

Fig. 6. Affine approximation for $y = \arctan x$.

When using the min-range approximation, the endpoint with the largest absolute value and the smallest slope is chosen as reference. Assuming that $|a| > |b|$, the parameters can be calculated as

$$\alpha = 1/(1 + a^2), \quad (77)$$

$$\beta = [\arctan a + \arctan b - \alpha(a + b)]/2, \quad (78)$$

$$\delta = [\arctan b - \arctan a - \alpha(b - a)]/2. \quad (79)$$

The result of the above approach is shown in Figure 6.

5.3.3 Examples for the Addition Operation.

Example 5.1. Four cases are implemented to show how the addition operation in PAA performs in this example.

A Part of MATLAB Code for Addition in PAA

```

function [addmag,addang]=addaff(xmag,xang,ymag,yang)
%initial parameters
pxmag=xmag;pxang=xang;pymag=ymag;pyang=yang;
%calculate the number of noisy symbols
xmnum=length(xmag);xanum=length(xang);
ymnum=length(ymag);yanum=length(yang);
a=max(xmnum,ymnum);b=max(xanum,xanum);
c=max(a,b);
[xmag,ymag]=conv(xmag,ymag);
x1=squareaff(xmag); % square of the magnitude
x2=squareaff(ymag);
for i=1:a
    x12(i)=x1(i)+x2(i);
end
x12(a+1)=abs(x1(a+1))+abs(x2(a+1));
ang=angdiff(xang,yang); %calculate θ
% multiplication of the magnitudes
[x3mag,x3ang]=multiplication(xmag,0,ymag,0);

```

<pre> x4=cosine(ang); %calculate cosθ [x5,x6]=sortaff(x3mag,x4); %multiplication of the magnitudes and cosθ [x7mag,x7ang]=multiplication(x5,0,x6,0); for i=1:c %summation operation x8(i)=x12(i)+2*x7mag(i); end x12l=length(x12); x7l=length(x7mag); d=max(x12l,x12l); [x12,x7mag]=conv(x12,x7mag); x8(c+1)=0; for i=c+1:d x8(c+1)=x8(c+1)+abs(x12(i))+2*abs(x7mag(i)); end %calculate magnitude of the result addmag=squarerootaff(x8);</pre>	<pre> x4=cosine(ang); %calculate cosθ [x5,x6]=sortaff(x3mag,x4); %multiplication of the magnitudes and cosθ [x7mag,x7ang]=multiplication(x5,0,x6,0); for i=1:c %summation operation x8(i)=x12(i)+2*x7mag(i); end x12l=length(x12); x7l=length(x7mag); d=max(x12l,x12l); [x12,x7mag]=conv(x12,x7mag); x8(c+1)=0; for i=c+1:d x8(c+1)=x8(c+1)+abs(x12(i))+2*abs(x7mag(i)); end %calculate magnitude of the result addmag=squarerootaff(x8);</pre>
---	---

In case 1, two complex fan variables are given as $\tilde{x} = [2, 4] \angle [\frac{5\pi}{18}, \frac{7\pi}{18}]$ and $\tilde{y} = [4, 6] \angle [\frac{\pi}{18}, \frac{\pi}{9}]$ with no dependency. Thus, the corresponding complex affine variables are given as $\hat{x} = (3 + \varepsilon_1) \angle (\frac{\pi}{3} + \frac{\pi}{18}\varepsilon_3)$ and $\hat{y} = (5 + \varepsilon_2) \angle (\frac{\pi}{12} + \frac{\pi}{36}\varepsilon_4)$.

Using PIA, the results of addition can be calculated as in Equation (80):

$$\tilde{z} = [5.5031, 9.4218] \angle [0.3435, 0.7854]. \quad (80)$$

Using PAA, the polar affine approximation for the addition of \hat{x} and \hat{y} is calculated as

$$\begin{aligned}
 \hat{z} = & (7.2378 + 0.9270\varepsilon_1 + 1.0143\varepsilon_2 - 0.2620\varepsilon_3 + 0.1310\varepsilon_4 + 0.5757\varepsilon_5) \\
 & \angle (0.5308 + 0.0639\varepsilon_1 - 0.0447\varepsilon_2 - 0.0666\varepsilon_3 + 0.0592\varepsilon_4 + 0.1986\varepsilon_6).
 \end{aligned} \quad (81)$$

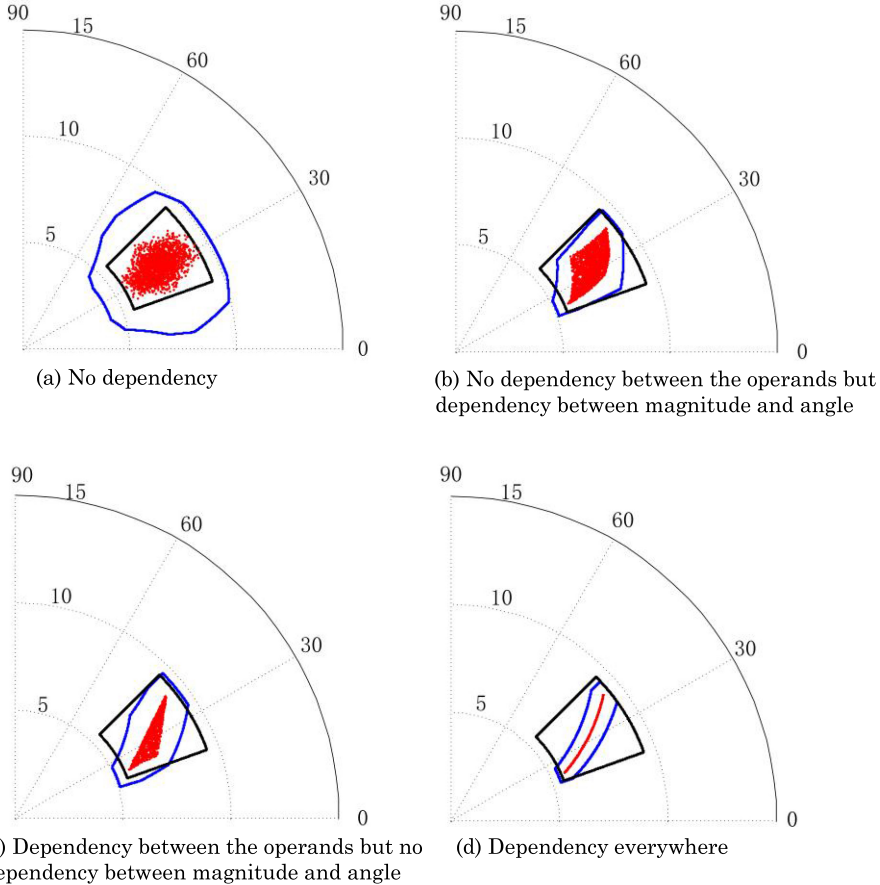


Fig. 7. Results of addition in PAA (blue line), PIA (black line), and actual solution (red dot).

The results of addition in PAA, PIA, and MC simulation are shown in Figure 7(a).

In case 2, there is no dependency between the operands, but dependency between magnitude and angle in each operand exists. Two complex affine variables are given as $\hat{x} = (3 + \varepsilon_1) \angle (\frac{\pi}{3} + \frac{\pi}{18}\varepsilon_2)$ and $\hat{y} = (5 + \varepsilon_2) \angle (\frac{\pi}{12} + \frac{\pi}{36}\varepsilon_1)$. The corresponding complex fan variables are the same as case 1.

The affine approximation for the addition of \hat{x} and \hat{y} is given as in Equation (82). The results of addition in PAA, PIA, and MC simulation are shown in Figure 7(b).

$$\begin{aligned} \hat{z} = & (7.3017 + 0.6494\varepsilon_1 + 1.1185\varepsilon_2 + 0.4462\varepsilon_3) \\ & \angle (0.5536 + 0.1268\varepsilon_1 + 0.0152\varepsilon_2 + 0.0743\varepsilon_4). \end{aligned} \quad (82)$$

In case 3, there is dependency between the operands, but no dependency between magnitude and angle in each operand exists. Two complex affine variables are given as $\hat{x} = (3 + \varepsilon_1) \angle (\frac{\pi}{3} + \frac{\pi}{18}\varepsilon_2)$ and $\hat{y} = (5 + \varepsilon_2) \angle (\frac{\pi}{12} + \frac{\pi}{36}\varepsilon_1)$. The affine approximation for the addition of \hat{x} and \hat{y} is given as in Equation (83). The results of addition in PAA, PIA, and MC simulation are shown in Figure 7(c).

$$\begin{aligned} \hat{z} = & (7.3214 + 1.0312\varepsilon_1 + 0.7332\varepsilon_2 + 0.4934\varepsilon_3) \\ & \angle (0.5346 + 0.1220\varepsilon_1 + 0.0233\varepsilon_2 + 0.0981\varepsilon_4). \end{aligned} \quad (83)$$

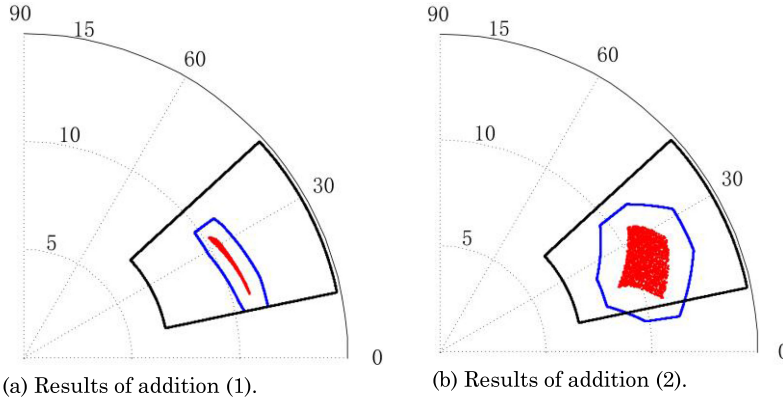


Fig. 8. Results of addition in PAA (blue line), PIA (black line), and actual solution (red dot).

In case 4, dependencies exist in both magnitude and angle. Two complex affine variables are given as $\hat{x} = (3 + \varepsilon_1) \angle (\frac{\pi}{3} + \frac{\pi}{18}\varepsilon_1)$ and $\hat{y} = (5 + \varepsilon_1) \angle (\frac{\pi}{12} + \frac{\pi}{36}\varepsilon_1)$. The affine approximation for the addition of \hat{x} and \hat{y} is given as in Equation (84). The results of addition in PAA, PIA, and MC simulation are shown in Figure 7(d):

$$\hat{z} = (7.3880 + 1.7474\varepsilon_1 + 0.2853\varepsilon_2) \angle (0.5453 + 0.1436\varepsilon_1 + 0.0645\varepsilon_3). \quad (84)$$

Example 5.2: Complicated dependency between two operands.

(1) The addition of two polar affine variables is given as

$$\hat{x} + \hat{y} = (3 + \varepsilon_1 + \varepsilon_2) \angle \left(\frac{5}{18}\pi - \frac{\pi}{18}\varepsilon_1 + \frac{\pi}{18}\varepsilon_2 \right) + (8 - \varepsilon_1 - \varepsilon_2) \angle \left(\frac{1}{12}\pi - \frac{\pi}{72}\varepsilon_1 + \frac{\pi}{72}\varepsilon_2 \right). \quad (85)$$

Compared with example 5.1, the dependency between the two polar affine variables becomes more complicated. Using the above approach, the polar affine variable \hat{z} of the addition operation is calculated as

$$\begin{aligned} \hat{z} = \hat{x} + \hat{y} &= (10.6616 + 0.0689\varepsilon_1 - 0.2519\varepsilon_2 + 0.5561\varepsilon_3) \\ &\angle (0.4196 - 0.0213\varepsilon_1 + 0.1318\varepsilon_2 + 0.0607\varepsilon_4). \end{aligned} \quad (86)$$

Figure 8(a) shows the solution regions of the results obtained from PAA, PIA, and MC simulations.

(2) Given the addition in polar affine form as

$$\hat{x} + \hat{y} = (3 + \varepsilon_1 + \varepsilon_2) \angle \left(\frac{5}{18}\pi - \frac{\pi}{18}\varepsilon_1 + \frac{\pi}{18}\varepsilon_2 \right) + (8 - 2\varepsilon_1) \angle \left(\frac{1}{12}\pi + \frac{\pi}{72}\varepsilon_1 + \frac{\pi}{72}\varepsilon_2 \right). \quad (87)$$

The affine approximation for the above addition operation is now calculated as

$$\begin{aligned} \hat{z} = \hat{x} + \hat{y} &= (10.5211 - 0.8261\varepsilon_1 + 0.7369\varepsilon_2 + 0.854\varepsilon_3) \\ &\angle (0.4083 + 0.0594\varepsilon_1 + 0.1171\varepsilon_2 + 0.0849\varepsilon_4). \end{aligned} \quad (88)$$

In this case, the coefficients of noisy symbol ε_1 in \hat{y} increase and change from positive correlation to negative correlation. The results are shown in Figure 8(b), which clearly demonstrates the advantages of PAA in the completeness property and the reduction of conservativeness.

The true solution regions are demonstrated by red dots in Figures 7 and 8. Figure 7(a) shows that the true solution region of the sum of two complex fans varying independently in their own ranges is not a complex fan. Furthermore, the true solution regions are various when different correlations exist in the operands. Thus, it is important to find the optimal solution region that

encompasses the true solution region. In these two examples of addition operation, the results from both PAA and PIA primarily contain all the true solutions from MC method, which guarantees the completeness property. Compared with PIA, it is noted that PAA shows its superiority when there is dependency between the operands or between magnitudes and angles. The solution regions of PAA are closer to the true solution regions than PIA when dependency exists. It is mainly because the operands in PIA are assumed to be independent and cannot reflect correlation information. In the single addition where there is absolutely no dependency, the solution region of PAA becomes wider because of the linear approximation in affine form. However, in practical examples, although the input variables are completely independent with each other, dependencies can arise from the calculation processes such as x/x , $(x+y)/(x-y)$, $x-x$, etc. In addition, the results obtained from PAA are all in linear representations, which is cheap to compute. Meanwhile, the solution region of PAA presents the similar shape as that of the true solution region due to the capability of keeping track of dependencies in the calculation process.

6 AA IN POLAR AND RECTANGULAR COORDINATES

This section mainly aims at analyzing the applicability of directly using PAA in polar coordinate systems. Both PAA and RAA inherit the advantages of AA. However, the characteristics of operations are different, while it is case specific to determine which representation is the most appropriate. As for case studies in polar coordinate systems with initial parameters in polar form, the polar form representation could be much more natural to users than the rectangular counterpart. Thus, if we still apply RAA to this case, then a conversion operation as that in Equation (90) is required to keep the initial dependencies among parameters. A comparison of PAA and RAA is carried out to demonstrate that the most appropriate choice is to directly use PAA in a polar coordinate system.

In PAA, multiplication and division do not cause difficulties but addition and subtraction are relatively complicated. The opposite situation occurs in RAA (Manson 2005).

Variables in polar affine form as in Equation (9) are first converted into the corresponding rectangular affine form as follows:

$$\hat{x}_R = x_0 + \sum_{i=1}^n x_i \varepsilon_i, \quad (89)$$

where x_0 and x_i are complex variables in rectangular form. ε_i are noisy symbols lying in $[-1, 1]$.

For comparing AA in polar and rectangular coordinates fairly, the conversion operations should primarily be presented for keeping consistent correlations among the variables. Given a polar affine variable \hat{x} in PAA as in Equation (9), it can be converted into the corresponding rectangular form as follows:

$$\hat{x}_R = \hat{x}_m \cos(\hat{x}_\alpha) + j \cdot \hat{x}_m \sin(\hat{x}_\alpha). \quad (90)$$

The problem in the conversion operation is similar as the addition operation in PAA due to the affine approximation for trigonometric function. Using the affine approximation method for trigonometric function in the above section, the complex variable in the corresponding rectangular form \hat{x}_R can be calculated. However, the conversion operation introduces new approximation errors and increases the complexity. A meaningful comparison is formulated to demonstrate that the most appropriate choice is to directly use PAA, instead of using RAA through a conversion operation in a polar coordinate system.

Given two complex variables in rectangular form, the addition and subtraction are presented in Equation (91):

$$\hat{x}_R \pm \hat{y}_R = (x_0 \pm y_0) + \sum_{i=1}^n (x_i \pm y_i) \varepsilon_i. \quad (91)$$

For a single addition/subtraction in PAA as in Equations (45)–(47), operations such as square operation, multiplication operation, square-root operation, as well as trigonometric and anti-trigonometric operations, all involve affine approximations. However, no affine approximation is required in RAA. Thus, addition and subtraction in RAA perform better with fewer approximations.

The result of multiplication (z_R) in Equation (92) is a non-affine quantity. The affine approximation for z_R is shown in Equations (93)–(95), where z_{real} and z_{imag} are real and imaginary approximation errors:

$$\begin{aligned} z_R &= \hat{x}_R \times \hat{y}_R = \left(x_0 + \sum_{i=1}^n x_i \varepsilon_i \right) \times \left(y_0 + \sum_{i=1}^n y_i \varepsilon_i \right) \\ &= x_0 y_0 + \sum_{i=1}^n (x_0 y_i + x_i y_0) \varepsilon_i + \left(\sum_{i=1}^n x_i \varepsilon_i \right) \times \left(\sum_{i=1}^n y_i \varepsilon_i \right), \end{aligned} \quad (92)$$

$$\hat{z}_R = \left(x_0 y_0 + \frac{1}{2} \sum_{i=1}^n x_i y_i \right) + \sum_{i=1}^n (x_0 y_i + x_i y_0) \varepsilon_i + z_{real} \varepsilon_{real} + j \cdot z_{imag} \varepsilon_{imag}, \quad (93)$$

$$z_{real} = \frac{1}{2} \sum_{i=1}^n |\operatorname{Re}(x_i y_i)| + \sum_{i=1}^n \sum_{j=i+1}^n |\operatorname{Re}(x_i y_j + x_j y_i)|, \quad (94)$$

$$z_{imag} = \frac{1}{2} \sum_{i=1}^n |\operatorname{Im}(x_i y_i)| + \sum_{i=1}^n \sum_{j=i+1}^n |\operatorname{Im}(x_i y_j + x_j y_i)|. \quad (95)$$

The division as shown in Equation (96) consists of multiplication and reciprocal operations in RAA:

$$\begin{aligned} \frac{\hat{x}_R}{\hat{y}_R} &= \frac{\operatorname{Re}(\hat{x}_R) + j \cdot \operatorname{Im}(\hat{x}_R)}{\operatorname{Re}(\hat{y}_R) + j \cdot \operatorname{Im}(\hat{y}_R)} = \frac{(\operatorname{Re}(\hat{x}_R) + j \cdot \operatorname{Im}(\hat{x}_R))(\operatorname{Re}(\hat{y}_R) - j \cdot \operatorname{Im}(\hat{y}_R))}{\operatorname{Re}(\hat{y}_R)^2 + \operatorname{Im}(\hat{y}_R)^2} \\ &= (\operatorname{Re}(\hat{x}_R) + j \cdot \operatorname{Im}(\hat{x}_R))(\operatorname{Re}(\hat{y}_R) - j \cdot \operatorname{Im}(\hat{y}_R)) \times \frac{1}{\operatorname{Re}(\hat{y}_R)^2 + \operatorname{Im}(\hat{y}_R)^2}. \end{aligned} \quad (96)$$

First, for a single multiplication in PAA as in Equations (16)–(21), one affine approximation for the third term in Equation (19) will introduce one error term (ε_k). It is mainly derived from $\varepsilon_i \varepsilon_j$ and ε_i^2 terms in Equation (19). Accordingly, for a single multiplication in RAA as in Equations (92)–(95), approximations in both real and imaginary components will introduce two error terms (ε_{real} , ε_{imag}). Second, for a single division in PAA as in Equations (27)–(29), two operations involve affine approximations, including one reciprocal operation and one multiplication operation. Accordingly, for a single division in RAA as in Equation (96), five operations involve affine approximations, including two square operations, one reciprocal operation, and two multiplication operations. Thus, multiplication and division in PAA perform better with fewer affine approximations.

Overall, the complexity of PAA is relatively higher by comprehensively comparing the four operations. More approximations exist in PAA due to the square-root operation as well as trigonometric and anti-trigonometric operations. However, the advantages and disadvantages of PAA and RAA are case specific. As for analyses of polar coordinate systems with initial parameters in polar form, the results show that the most appropriate choice is to directly use PAA. Meanwhile, case studies in Sections 6 and 7 can support directly using PAA in polar coordinate systems.

Example 6.1. Given two polar affine variables (full AA) as $\hat{x} = (4 + 2\varepsilon_1) \angle (\frac{\pi}{12} + \frac{\pi}{18}\varepsilon_1)$ and $\hat{y} = (8 + 2\varepsilon_1) \angle (\frac{2\pi}{9} + \frac{\pi}{18}\varepsilon_1)$ in example 4.1. In this example, the comparison of multiplication in PAA and RAA is implemented. The division is similar except it involves the reciprocal operation.

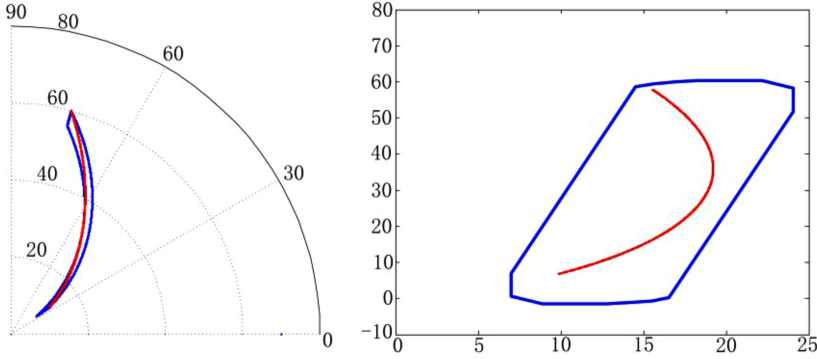


Fig. 9. Comparison of multiplication in PAA and RAA (blue line) with actual solution (red dot).

First, \hat{x} and \hat{y} are converted into the corresponding variables \hat{x}_R and \hat{y}_R in rectangular form as shown in Equations (97) and (98).

$$\hat{x}_R = (3.7895 + 1.7376\epsilon_1 + 0.0887\epsilon_2) + j \cdot (1.1953 + 1.1846\epsilon_1 + 0.1797\epsilon_3), \quad (97)$$

$$\hat{y}_R = (5.9700 + 0.6276\epsilon_1 + 0.1696\epsilon_4) + j \cdot (5.2362 + 2.3398\epsilon_1 + 0.1820\epsilon_5). \quad (98)$$

Then, the multiplication of \hat{x} and \hat{y} is calculated as

$$\begin{aligned} \hat{z}_R = & (15.5239 + 3.7522\epsilon_1 + 0.5295\epsilon_2 - 0.9409\epsilon_3 + 0.6427\epsilon_4 + 0.6897\epsilon_5 + 1.9589\epsilon_6) \\ & + j \cdot (29.3831 + 25.7873\epsilon_1 + 0.4645\epsilon_2 + 1.0728\epsilon_3 + 0.2027\epsilon_4 + 0.2175\epsilon_5 + 3.2046\epsilon_7). \end{aligned} \quad (99)$$

The solution region of the result in Equation (99) is demonstrated in Figure 9. The corresponding result of PAA is obtained from example 4.1.

Example 6.2. Given two polar affine variables (full AA) as $\hat{x} = (3 + \epsilon_1) \angle (\frac{\pi}{3} + \frac{\pi}{18}\epsilon_1)$ and $\hat{y} = (5 + \epsilon_1) \angle (\frac{\pi}{12} + \frac{\pi}{36}\epsilon_1)$ in example 5.1, the comparison of addition in PAA and RAA is implemented. The subtraction is the combination of addition and negation.

First, \hat{x} and \hat{y} are converted into the corresponding variables \hat{x}_R and \hat{y}_R in rectangular form as shown in Equations (100) and (101).

$$\hat{x}_R = (1.4134 + 0.0450\epsilon_1 + 0.0904\epsilon_2) + j \cdot (2.6216 + 1.1198\epsilon_1 + 0.0698\epsilon_3), \quad (100)$$

$$\hat{y}_R = (4.8092 + 0.8511\epsilon_1 + 0.0221\epsilon_4) + j \cdot (1.3336 + 0.6793\epsilon_1 + 0.0451\epsilon_5). \quad (101)$$

Then, the addition of \hat{x} and \hat{y} is calculated as

$$\begin{aligned} \hat{z}_R = & (6.2226 + 0.8961\epsilon_1 + 0.0904\epsilon_2 + 0.0221\epsilon_4) \\ & + j \cdot (3.9552 + 1.7991\epsilon_1 + 0.0698\epsilon_3 + 0.0451\epsilon_5). \end{aligned} \quad (102)$$

Figure 10 shows the solution region of addition in polar and rectangular coordinates. The result of addition in PAA is obtained from example 5.1.

By comparing the calculation process and the results of PAA and RAA, it demonstrates that they both have the capability of tracing dependencies among the variables. It is noted that the advantages of AA exist in both PAA and RAA. However, operations in PAA and RAA have different characteristics. Although the overall complexity of PAA is relatively higher than that of RAA, the results show that the most appropriate choice is to directly use PAA in such a polar coordinate system with initial parameters in polar form. Figure 9 shows a comparison of solution regions of multiplication in PAA and RAA. It is observed that PAA performs better with more accurate results in such a case. The reasons are that: (i) multiplication in PAA involves fewer approximations

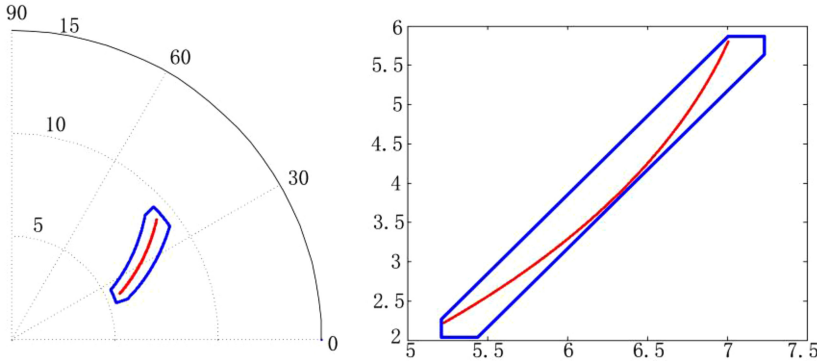


Fig. 10. Comparison of addition in PAA and RAA (blue line) with actual solution (red dot).

than that in RAA, as described above; and (ii) new approximation errors have been introduced by the conversion operation. Figure 10 shows a comparison of solution regions of addition in PAA and RAA. It is observed that RAA is slightly more accurate than PAA. Indeed, as for a single addition operation, PAA has a much higher degree of approximation than RAA. However, in such a polar coordinate system, the use of RAA requires a conversion operation as in Equation (90), which introduces new approximation errors and increases computational complexity. Thus, PAA only presents slightly less accuracy than RAA. The results demonstrate that the most appropriate choice is to directly use PAA in a polar coordinate system. In addition, an application of PAA in circuit analysis is presented in Section 7 to support directly using PAA in polar coordinate systems.

7 CASE STUDY

For circuit analysis in the field of electrical engineering, parameters are commonly characterized by phasors. A phasor is defined as a variable with magnitude and angle, which is a typical complex variable in polar form. For example, parameters such as voltages, currents, and impedances are commonly represented by phasors in circuit analysis. Thus, the initial parameters in polar form contribute to directly using PAA in this case. Figure 11 shows an $R-L$ circuit operated in the steady state. In practice, data errors are inevitable in the calculation process because of the operating environment, measuring errors, and component materials. PAA provides an effective means for representing phasors under uncertainty and computing the parameters while considering the correlations among the same kind of elements operated in the same environment. The simulation case is close to the operation of a practical circuit in the field of electrical engineering. The use of PAA can reflect the impacts of multiple uncertainties on different type of elements in the circuit.

As for the circuit model in Figure 11, parameters are calculated as in Equations (103)–(107) based on the typical circuit theory. For example, the impedance of series cluster Z_1 can be calculated by combining the resistances R_1 and R_2 as well as the impedance Z_2 . The branch currents I_{R1} , I_{R2} , I_{Z3} , and I_{Z4} can be calculated by the current diffusion of the current source I_S :

$$Z_{1m} \angle Z_{1\alpha} = \frac{Z_{R_1m} \angle Z_{R_1\alpha} \times Z_{R_2m} \angle Z_{R_2\alpha}}{Z_{R_1m} \angle Z_{R_1\alpha} + Z_{R_2m} \angle Z_{R_2\alpha}} + Z_{2m} \angle Z_{2\alpha}, \quad (103)$$

$$I_{R_1m} \angle I_{R_1\alpha} = \frac{Z_{R_2m} \angle Z_{R_2\alpha}}{Z_{R_1m} \angle Z_{R_1\alpha} + Z_{R_2m} \angle Z_{R_2\alpha}} \times I_{Sm} \angle I_{S\alpha}, \quad (104)$$

$$I_{R_2m} \angle I_{R_2\alpha} = \frac{Z_{R_1m} \angle Z_{R_1\alpha}}{Z_{R_1m} \angle Z_{R_1\alpha} + Z_{R_2m} \angle Z_{R_2\alpha}} \times I_{Sm} \angle I_{S\alpha}, \quad (105)$$

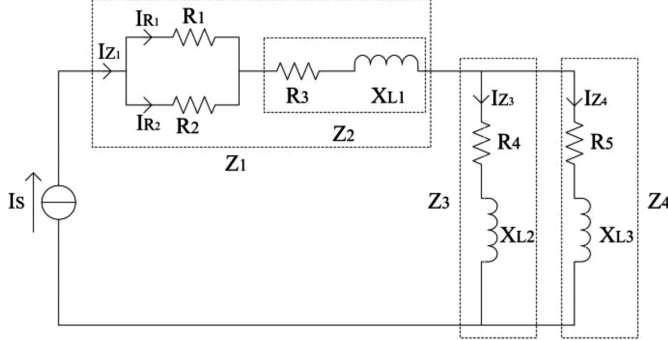


Fig. 11. R-L circuit operated in the steady state.

$$IZ_{3m} \angle Z_{3\alpha} = \frac{Z_{4m} \angle Z_{4\alpha}}{Z_{3m} \angle Z_{3\alpha} + Z_{4m} \angle Z_{4\alpha}} \times ISm \angle IS\alpha, \quad (106)$$

$$IZ_{4m} \angle Z_{4\alpha} = \frac{Z_{3m} \angle Z_{3\alpha}}{Z_{3m} \angle Z_{3\alpha} + Z_{4m} \angle Z_{4\alpha}} \times ISm \angle IS\alpha. \quad (107)$$

Quantitative computation is then carried out for circuit analysis in Figure 11. The capability of tracing dependencies among variables also reflects the suitability of PAA in this case. All elements in the circuit are operated in the same environment over certain time periods. Uncertainties would arise from the measuring errors, environment disturbance, and component materials, and so on. However, different types of elements present different levels of sensitivities to multiple uncertainties in the operating environment. Accordingly, in AA, ε is used to represent the impact factor and the corresponding coefficient is used to reflect the degree of impacts on a specific element. The current source is initialized as $\hat{IS}_m \angle \hat{IS}\alpha = (10 + \varepsilon_S) \angle (\frac{1}{36}\pi + \frac{1}{36}\pi\varepsilon_S)$ affected by the noisy symbol ε_S . It is mainly affected by changes in ambient temperature. Thus, ε_S is used to represent this main impact factor, and the corresponding coefficients in magnitude and angle reflect the degree of the impact on the current source. The resistances are initialized as $\hat{Z}_{R_1m}^P = 6 + \varepsilon_1$, $\hat{Z}_{R_1\alpha}^P = 0$, $\hat{Z}_{R_2m}^P = 11 + \varepsilon_1$, $\hat{Z}_{R_2\alpha}^P = 0$. The dependency among resistances is characterized by ε_1 . As for the resistances such as R_1 and R_2 , they are mainly affected by the measuring error introduced by the resistance meter. Assuming that resistances in the circuit are measured with the same resistance meter, ε_1 is used to represent this main impact factor and the corresponding coefficient in each resistance reflects the degree of the impact on each resistance. The initial impedances in polar affine form are shown in Equations (108)–(110). The presence of ε_1 and ε_2 is arising from the dependency among resistances and reactances, respectively:

$$\hat{Z}_{2m}^P \angle \hat{Z}_{2\alpha}^P = (5 + \varepsilon_1 + \varepsilon_2) \angle \left(\frac{5}{36}\pi + \frac{1}{60}\pi\varepsilon_1 + \frac{1}{90}\pi\varepsilon_2 \right), \quad (108)$$

$$\hat{Z}_{3m}^P \angle \hat{Z}_{3\alpha}^P = (5.5 + \varepsilon_1 + 0.5\varepsilon_2) \angle \left(\frac{1}{6}\pi + \frac{1}{24}\pi\varepsilon_1 + \frac{1}{72}\pi\varepsilon_2 \right), \quad (109)$$

$$\hat{Z}_{4m}^P \angle \hat{Z}_{4\alpha}^P = (11 + 0.5\varepsilon_1 + 0.5\varepsilon_2) \angle \left(\frac{31}{72}\pi + \frac{1}{36}\pi\varepsilon_1 + \frac{1}{72}\pi\varepsilon_2 \right). \quad (110)$$

Then, a comprehensive comparison is formulated by using both PAA and RAA in this case. A conversion operation is required in a polar coordinate system with initial parameters in polar form. Thus, the corresponding parameters in rectangular affine form are obtained by Equation (90).

The resistances in rectangular affine form are $\hat{Z}_{R_1}^R = 6 + \varepsilon_1$ and $\hat{Z}_{R_2}^R = 11 + \varepsilon_1$. The corresponding current source and impedances are shown as in Equations (111)–(114):

$$\hat{I}_S^R = (9.9392 + 0.9183\varepsilon_S + 0.0246\varepsilon_{S,1}) + j \cdot (0.9134 + 0.9552\varepsilon_S + 0.0453\varepsilon_{S,2}), \quad (111)$$

$$\begin{aligned} \hat{Z}_2^R &= (4.5045 + 0.7941\varepsilon_1 + 0.8309\varepsilon_2 + 0.0673\varepsilon_{Z_{2,1}}) \\ &\quad + j \cdot (2.1486 + 0.6588\varepsilon_1 + 0.5798\varepsilon_2 + 0.1241\varepsilon_{Z_{2,2}}), \end{aligned} \quad (112)$$

$$\begin{aligned} \hat{Z}_3^R &= (4.6890 + 0.5013\varepsilon_1 + 0.3103\varepsilon_2 + 0.1383\varepsilon_{Z_{3,1}}) \\ &\quad + j \cdot (2.7950 + 1.1165\varepsilon_1 + 0.4549\varepsilon_2 + 0.1864\varepsilon_{Z_{3,2}}), \end{aligned} \quad (113)$$

$$\begin{aligned} \hat{Z}_4^R &= (2.3389 - 0.8267\varepsilon_1 - 0.3595\varepsilon_2 + 0.1068\varepsilon_{Z_{4,1}}) \\ &\quad + j \cdot (10.7004 + 0.6932\varepsilon_1 + 0.5896\varepsilon_2 + 0.0713\varepsilon_{Z_{4,2}}). \end{aligned} \quad (114)$$

PIA is also applied to the circuit analysis for comparison. The initial parameters are represented by the corresponding polar interval forms. The current source is $\tilde{I}_{Sm}^P \angle \tilde{I}_{S\alpha}^P = [9, 11] \angle [0, \pi/18]$. The resistances are $\tilde{Z}_{R_1m}^P = [5, 7]$, $\tilde{Z}_{R_1\alpha}^P = [0, 0]$, $\tilde{Z}_{R_2m}^P = [10, 12]$, and $\tilde{Z}_{R_2\alpha}^P = [0, 0]$. The impedances are shown in Equations (115)–(117):

$$\tilde{Z}_{2m}^P \angle \tilde{Z}_{2\alpha}^P = [3, 7] \angle \left[\frac{1}{9}\pi, \frac{1}{6}\pi \right], \quad (115)$$

$$\tilde{Z}_{3m}^P \angle \tilde{Z}_{3\alpha}^P = [4, 7] \angle \left[\frac{1}{9}\pi, \frac{2}{9}\pi \right], \quad (116)$$

$$\tilde{Z}_{4m}^P \angle \tilde{Z}_{4\alpha}^P = [10, 12] \angle \left[\frac{7}{18}\pi, \frac{17}{36}\pi \right]. \quad (117)$$

Accordingly, interval arithmetic in rectangular form (RIA) is also applied to demonstrate the superiority of AA. The current source in rectangular interval form is $\tilde{I}_S^R = [8.8633, 11] + j \cdot [0, 1.9101]$. The resistances in rectangular interval form are $\tilde{Z}_{R_1}^R = [5, 7]$ and $\tilde{Z}_{R_2}^R = [10, 12]$. The corresponding impedances are shown in Equations (118)–(120):

$$\tilde{Z}_2^R = [2.5981, 6.5778] + j \cdot [1.0261, 3.5], \quad (118)$$

$$\tilde{Z}_3^R = [3.0642, 6.5778] + j \cdot [1.3681, 4.4995], \quad (119)$$

$$\tilde{Z}_4^R = [0.8716, 4.1042] + j \cdot [9.3969, 11.9543]. \quad (120)$$

The results of impedance Z_1 using PAA and RAA are calculated as

$$\begin{aligned} \tilde{Z}_{1m}^P \angle \tilde{Z}_{1\alpha}^P &= (8.5882 + 1.5103\varepsilon_1 + 0.9837\varepsilon_2 + 0.1269\varepsilon_{Z_{1,1}} + 0.4113\varepsilon_{Z_{1,2}}) \\ &\quad \angle (0.2483 + 0.0350\varepsilon_1 + 0.0415\varepsilon_2 - 0.0039\varepsilon_{Z_{1,1}} + 0.0731\varepsilon_{Z_{1,3}}), \end{aligned} \quad (121)$$

$$\begin{aligned} \hat{Z}_1^R &= (8.3840 + 1.3344\varepsilon_1 + 0.8309\varepsilon_2 + 0.1949\varepsilon_{Z_{1,4}}) \\ &\quad + j \cdot (2.1486 + 0.6588\varepsilon_1 + 0.5798\varepsilon_2 + 0.1241\varepsilon_{Z_{2,2}}). \end{aligned} \quad (122)$$

The corresponding results using PIA and RIA are calculated as

$$\tilde{Z}_{1m}^P \angle \tilde{Z}_{1\alpha}^P = [5.4404, 12.4110] \angle [0.1213, 0.3827], \quad (123)$$

$$\tilde{Z}_1^R = [5.2297, 12.1778] + j \cdot [1.0261, 3.5]. \quad (124)$$

The solution regions of impedance Z_1 in both polar and coordinates are shown in Figure 12. The results obtained by interval arithmetic and affine arithmetic are depicted with black lines and blue lines, respectively. Meanwhile, the MC sampling method is also used to obtain the corresponding true solution regions (red dot).

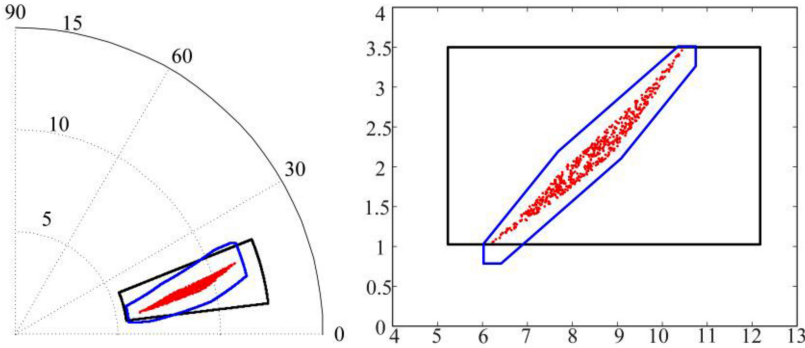


Fig. 12. Solution regions of Z_1 by AA (blue line), IA (black line), and MC method (red dot).

Table 1. Comparison on Bounds of the Results Obtained from PAA and PIA

Bounds of the results converted from PAA	Bounds of the results obtained from PIA
$\tilde{I}_{R_1 m}^P \angle \tilde{I}_{R_1 \alpha}^P = [5.5422, 7.4118] \angle [0, \pi/18]$	$\tilde{I}_{R_1 m}^P \angle \tilde{I}_{R_1 \alpha}^P = [4.7367, 8.8] \angle [0, \pi/18]$
$\tilde{I}_{R_2 m}^P \angle \tilde{I}_{R_2 \alpha}^P = [2.9068, 4.1272] \angle [0, \pi/18]$	$\tilde{I}_{R_2 m}^P \angle \tilde{I}_{R_2 \alpha}^P = [2.3679, 5.1337] \angle [0, \pi/18]$
$\tilde{I}_{Z_3 m}^P \angle \tilde{I}_{Z_3 \alpha}^P = [5.6977, 8.8803] \angle [0.2096, 0.5214]$	$\tilde{I}_{Z_3 m}^P \angle \tilde{I}_{Z_3 \alpha}^P = [4.8915, 10.7855] \angle [-0.0733, 0.7906]$
$\tilde{I}_{Z_4 m}^P \angle \tilde{I}_{Z_4 \alpha}^P = [2.5253, 4.7047] \angle [-0.6630, -0.2640]$	$\tilde{I}_{Z_4 m}^P \angle \tilde{I}_{Z_4 \alpha}^P = [1.9566, 6.2920] \angle [-0.9460, 0.0052]$

Table 2. Comparison on Bounds of the Results Obtained from RAA and RIA

Bounds of the results converted from RAA	Bounds of the results obtained from RIA
$\tilde{I}_{R_1}^R = [5.5426, 7.3400] + j \cdot [-0.1070, 1.2910]$	$\tilde{I}_{R_1}^R = [4.6649, 8.8000] + j \cdot [0, 1.5281]$
$\tilde{I}_{R_2}^R = [2.9100, 4.0852] + j \cdot [-0.0755, 0.7183]$	$\tilde{I}_{R_2}^R = [2.3324, 5.1333] + j \cdot [0, 0.8914]$
$\tilde{I}_{Z_3}^R = [3.6427, 10.3399] + j \cdot [0.3306, 4.8956]$	$\tilde{I}_{Z_3}^R = [0.6888, 20.5840] + j \cdot [-2.5575, 13.4038]$
$\tilde{I}_{Z_4}^R = [0.6463, 5.9419] + j \cdot [-2.9646, -0.3712]$	$\tilde{I}_{Z_4}^R = [0.3976, 13.5776] + j \cdot [-8.6108, 3.3609]$

In this circuit model, current diffusion of the parallel components R_1 and R_2 as well as Z_3 and Z_4 are calculated in PAA and PIA, respectively. According to the basic circuit theory shown in Equations (104)–(107), the results of individual branch currents in PAA are calculated as in Equations (125)–(128). The branch currents in polar affine form can be converted into the corresponding polar interval form via conversion operation for intuitive comparison. Table 1 compares bounds of the results obtained from the conversion of PAA with those from PIA. Accordingly, Table 2 compares bounds of the results obtained from the conversion of RAA with those from RIA:

$$\hat{I}_{R_1 m}^P \angle \hat{I}_{R_1 \alpha}^P = (6.4770 - 0.1780\epsilon_1 + 0.6477\epsilon_S + 0.1091\epsilon_{R_1,1}) \angle \left(\frac{1}{36}\pi + \frac{1}{36}\pi\epsilon_S\right), \quad (125)$$

$$\hat{I}_{R_2 m}^P \angle \hat{I}_{R_2 \alpha}^P = (3.5170 + 0.1720\epsilon_1 + 0.3517\epsilon_S + 0.0865\epsilon_{R_2,1}) \angle \left(\frac{1}{36}\pi + \frac{1}{36}\pi\epsilon_S\right), \quad (126)$$

$$\begin{aligned} \hat{I}_{Z_3 m}^P \angle \hat{I}_{Z_3 \alpha}^P &= (7.2890 - 0.3820\epsilon_1 - 0.1070\epsilon_2 + 0.7289\epsilon_S + 0.3734\epsilon_{Z_3,3}) \\ &\quad \angle (0.3655 + 0.0089\epsilon_1 + 0.0069\epsilon_2 + 0.0873\epsilon_S + 0.0528\epsilon_{Z_3,4}), \end{aligned} \quad (127)$$

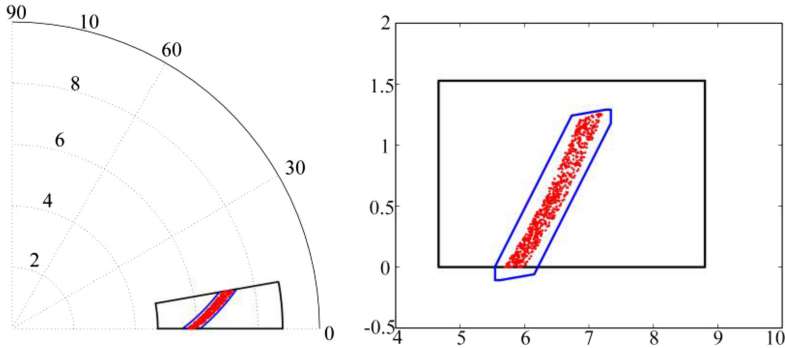


Fig. 13. Solution regions of I_1 by AA (blue line), IA (black line), and MC method (red dot).

$$\begin{aligned} \hat{I}_{Z_4 m}^P \angle \hat{I}_{Z_4 \alpha}^P = & (3.6150 + 0.3080\epsilon_1 + 0.1130\epsilon_2 + 0.3615\epsilon_S + 0.3072\epsilon_{Z_4,3}) \\ & \angle (-0.4635 + 0.0525\epsilon_1 + 0.0069\epsilon_2 + 0.0873\epsilon_S + 0.0528\epsilon_{Z_4,4}). \end{aligned} \quad (128)$$

Taking the results of branch current I_1 as an example, the solution regions in both polar and rectangular coordinates are shown in Figure 13. Similarly, the results obtained by interval arithmetic and affine arithmetic are, respectively, depicted with black lines and blue lines. The corresponding true solution regions obtained by the MC sampling method are depicted with red dots.

First, it is observed that AA shows significant advantages over IA and MC methods in both polar and rectangular coordinates. Tables 1 and 2 demonstrate that the bounds of branch currents obtained by AA are much tighter than those obtained by IA. Meanwhile, the boundary of AA is closer to the true solution region when compared with that of IA in Figures 12 and 13. Thus, AA is less conservative than IA and also guarantees the completeness of true solutions when compared with the MC sampling method. In both polar and rectangular coordinates, AA can reflect the dependency among the same elements (I_S , R , or X) while IA can only show variation ranges of individual parameters. For example, when calculating branch current, numerator and denominator of $Z_{R2}/(Z_{R1}+Z_{R2})$ are dependent because of the common term Z_{R2} . In AA, this dependency is reflected by the common noisy symbols in numerator and denominator. However, numerator and denominator are still assumed to vary independently in their own ranges in IA. Thus, AA provides better results than IA in both polar and rectangular coordinates.

Second, the comparisons of the calculation process as well as the solution regions as shown in Figures 12 and 13 demonstrate that a more appropriate choice is to directly use PAA in this case. In such a polar coordinate system with initial parameters in polar form, a conversion operation as in Equation (90) is required when calculating via RAA. The conversion operation keeps the initial dependencies among parameters but introduces new approximation errors and increases the complexity. In Figure 12, the solution regions of Z_1 obtained by both PAA and RAA are close to the true solution regions. In addition, it is observed that degrees of closeness are basically the same. When calculating Z_1 via Equation (103), the first terms in PAA and RAA are the same, because angles of resistances are 0. RAA has a computational advantage due to the addition operation in Equation (103). However, the conversion operation introduces new approximation errors in such a polar coordinate system. Thus, degrees of closeness to the true solution regions are basically the same as shown in Figure 12. Meanwhile, Figure 13 demonstrates that the solution region obtained by PAA is relatively closer to the true solution region than that obtained by RAA. The reasons are: (i) multiplication and division in PAA perform better with fewer approximations, and (ii) directly using PAA avoids new approximation errors introduced by the conversion operation. In summary, a more appropriate choice is to directly use PAA in a polar coordinate system.

8 CONCLUSIONS

This article provides an explicit definition on the polar affine arithmetic, which is an extension of affine arithmetic to the polar coordinate systems. Basic arithmetic operations including addition, subtraction, multiplication, and division are developed based on the complex affine arithmetic. The algorithms are presented in MATLAB programs. The addition of variables in polar form is always the most complicated part in existing studies. A traditional method is to convert complex variables in polar form to rectangular or circular form, which may derive conservative results due to the conversion. Polar interval arithmetic is developed as a means for providing the smallest complex fan that encloses all possible results. The results of the operations in PAA, PIA, and MC method are compared in quantitative examples. Four cases are designed to show how the proposed PAA performs with respect to different dependency situations, i.e., no dependency at all, dependency only existing between angle and magnitude, dependency only existing between the operands, and dependency everywhere. In a single operation, the results show that when dependency exists, the solution regions from PAA are closer to the true solution regions than those from PIA. Unlike PIA, the profile of the solution region in PAA that encloses the possible results is not limited to the complex fan shape. When there is absolutely no dependency, the results show that the solution region of PAA becomes wider because of the linear approximation in affine form. However, in practical examples, although the input variables could be completely independent with each other, dependencies can arise from the calculation processes such as x/x , $(x+y)/(x-y)$, $x-x$, etc. Thus, the superiority of PAA is observed when dependencies exist in input variables and/or arise from the calculation process.

Since the affine arithmetic in rectangular coordinates also has the similar capability as in polar coordinates, a comparison of PAA and RAA is further presented. The advantages and disadvantages of using either polar or rectangular representation are certainly case specific. Case study shows an application of PAA to the analysis of an $R-L$ circuit operated in the steady state. PAA takes account of the dependency among the same elements under uncertainty, while PIA can only show variation ranges of individual variables. Thus, PAA keeps track of dependency throughout the calculation process, and in turn performs better in this case. A comparison of RAA and PAA is further carried out to demonstrate that the more appropriate choice is to directly use PAA in a polar coordinate system. PAA proves to be valuable in certain cases while PIA does not work well due to the conservativeness. Furthermore, potential applications of PAA in other research fields involving complex variables in polar form will be gradually developed.

ACKNOWLEDGMENTS

The authors would like to thank Tianjin University for providing facilities and scientific environment for our research.

REFERENCES

- G. Alefeld and G. Mayer. 2000. Interval analysis: Theory and applications. *J. Comput. Appl. Math.* 121, 1 (2000), 421–464.
- R. E. Boche. 1966. Complex interval arithmetic with some applications. Lockheed Missiles and Space Company Report 4-22-66-1. 1–31.
- Y. Candau, T. Raissi, N. Ramdani, and L. Ibos. 2006. Complex interval arithmetic using polar form. *Reliable Comput.* 12, 1 (2006), 1–20.
- C. Cui and K. N. Ngan. 2011. Scale-and affine-invariant fan feature. *IEEE Trans. Image Process.* 20, 6 (2011), 1627–1640. DOI : [10.1109/TIP.2010.2103948](https://doi.org/10.1109/TIP.2010.2103948)
- T. Ding, H. Cui, and W. Gu. 2012. An uncertainty power flow algorithm based on interval and affine arithmetic. *Auto. Elect. Power Syst.* 36, 13 (2012), 51–55.
- C. Doerr. 2013. Challenge tracing and mitigation under partial information and uncertainty. In *Proceedings of the CNS-IEEE*. 446–453. DOI : [10.1109/CNS.2013.6682759](https://doi.org/10.1109/CNS.2013.6682759)
- R. T. Farouki and H. Pottmann. 2002. Exact minkowski products of N complex disks. *Reliable Comput.* 8 (2002), 43–66.

- S. E. Ferrando, L. A. Kolasa, and N. Kovacevic. 2002. Algorithm 820: A flexible implementation of matching pursuit for Gabor functions on the interval. *ACM Trans. Math. Softw.* 28, 3 (2002), 337–353. DOI : [10.1145/569147.569151](https://doi.org/10.1145/569147.569151)
- L. D. Figueiredo, R. V. Iwaarden, and J. Stolfi. 1997. Fast interval branch-and-bound methods for unconstrained global optimization with affine arithmetic. Institute of Computing, University of Campinas, Rapport technique IC-9708.
- J. Flores. 1999. Complex fans: A representation for vectors in polar form with interval attributes. *ACM Trans. Math. Softw.* 25, 2 (1999), 129–156. DOI : [10.1145/317275.317277](https://doi.org/10.1145/317275.317277)
- I. Gargantini and P. Henrici. 1971. Circular arithmetic and the determination of polynomial zeros. *Springer Lecture Notes* 228 (1971), 86–92.
- L. Granvilliers and F. Benhamou. 2006. Algorithm 852: RealPaver: An interval solver using constraint satisfaction techniques. *ACM Trans. Math. Softw.* 32, 1 (2006), 138–156. DOI : [10.1145/1132973.1132980](https://doi.org/10.1145/1132973.1132980)
- W. Heupke, C. Grimm, and K. Waldschmidt. 2006. Modeling uncertainty in nonlinear analog systems with Affine arithmetic. In *Proceedings of the Applications of Specification and Design Languages for SoCs: Selected Papers from FDL 2005*. 155.
- R. Klatte and Ch. Ullrich. 1980. Complex sector arithmetic. *Computing* 24, 2–3 (1980), 139–148.
- J. Luiz, D. Comba, and J. Stolfi. 1993. Affine arithmetic and its applications to computer graphics. In *Proceedings of the Brazilian Symposium on Computer Graphics and Image*. 9–18.
- G. Manson. 2005. Calculating frequency response functions for uncertain systems using complex affine analysis. *J. Sound Vibrat.* 288, 3 (2005), 487–521. DOI : [10.1016/j.jsv.2005.07.004](https://doi.org/10.1016/j.jsv.2005.07.004)
- R. E. Moore. 1962. Interval arithmetic and automatic error analysis in digital computing. *Stanford University of California Applied Mathematics and Statistics Labs*.
- N. R. Pal and J. C. Bezdek. 1994. Measuring fuzzy uncertainty. *IEEE Trans. Fuzzy Syst.* 2, 2 (1994), 107–118. DOI : [10.1109/91.277960](https://doi.org/10.1109/91.277960)
- M. S. Petković and L. D. Petković. 1998. *Complex Interval Arithmetic and Its Applications*. Wiley-VCH, Berlin, 1998.
- A. Piccolo, A. Vaccaro, and D. Villacci. 2013. An affine arithmetic-based methodology for the thermal rating assessment of overhead lines in the presence of Data Uncertainty. In *Proceedings of the IEEE Power Tech Conference*. 324–331. DOI : [10.1109/PTC.2003.1304743](https://doi.org/10.1109/PTC.2003.1304743)
- G. Rao, S. Singiresu, and L. Berke. 2010. Analysis of uncertain structural systems using interval analysis. *AIAA J.* 35, 4 (2010), 727–735.
- P. Saracco and M. G. Pia. 2013. Progress with uncertainty quantification in generic Monte Carlo simulations. In *Proceedings of the NSS/MIC-IEEE*. 1–6. DOI : [10.1109/NSSMIC.2013.6829453](https://doi.org/10.1109/NSSMIC.2013.6829453)
- J. Stol and L. H. De Figueiredo. 1997. Self-validated numerical methods and applications. *Monograph for 21st Brazilian Mathematics Colloquium (IMPA'97)*. Citeseer, vol. 5, 1.
- A. Vaccaro, C. A. Canizares, and D. Villacci. 2010. An affine arithmetic-based methodology for reliable power flow analysis in the presence of data uncertainty. *IEEE Trans. Power Syst.* 25, 2 (2010), 624–632. DOI : [10.1109/TPWRS.2009.2032774](https://doi.org/10.1109/TPWRS.2009.2032774)
- S. Wang, L. Han, and L. Wu. 2015. Uncertainty tracing of distributed generations via complex affine arithmetic-based unbalanced three-phase power flow. *IEEE Trans. Power Syst.* 30, 6 (2015), 3053–3062. DOI : [10.1109/TPWRS.2014.2377042](https://doi.org/10.1109/TPWRS.2014.2377042)
- S. Wang, M. Chen, C. Wang, and G. Zhang. 2006. Interval power flow analysis with complex-fan representation for distribution networks. In *Proceedings of the China International Conference on Electricity Distribution (CICED'06)*. 116–122. DOI : [10.1049/cp:20061751](https://doi.org/10.1049/cp:20061751)
- K. L. Wood, K. N. Otto, and E. K. Antonsson. 1992. Engineering design calculations with fuzzy parameters. *Fuzzy Sets Syst.* 52, 1 (1992), 1–20. DOI : [10.1016/0165-0114\(92\)90031-X](https://doi.org/10.1016/0165-0114(92)90031-X)
- H. Wu and J. M. Mendel. 2002. Uncertainty bounds and their use in the design of interval type-2 fuzzy logic systems. *IEEE Trans. Fuzzy Syst.* 10, 5 (2002), 622–639. DOI : [10.1109/TFUZZ.2002.803496](https://doi.org/10.1109/TFUZZ.2002.803496)

Received June 2016; revised May 2018; accepted August 2018